Intestinal GCN2 controls Drosophila systemic growth upon AA imbalance in response to Lactiplantibacillus plantarum symbiotic cues encoded by r/tRNA operons

Grenier T.[1], Consuegra J.[1], Matos RC.[1], Akherraz H.[1], Gillet B.[1], Hugues S.[1], Leulier F[1*].

[1.] Institut de Génomique Fonctionnelle de Lyon (IGFL), Ecole Normale Supérieure de Lyon, CNRS UMR 5242, Université Claude Bernard Lyon 1, 69364 Lyon Cedex 07, France
*corresponding author: francois.leulier@ens-lyon.fr

Abstract

Symbiotic bacteria support host growth upon malnutrition. How bacteria achieve this remains partly elusive. Here, we took advantage of the mutualism between Drosophila and *Lactiplantibacillus plantarum* (Lp) to investigate such mechanisms. Using chemically-defined holidic diets, we found that association with Lp improves the growth of larvae fed amino acid-imbalanced diets. We show that in this context Lp supports its host's growth through a molecular dialog that requires functional operons encoding ribosomal and transfer RNAs (r/tRNAs) in Lp and the GCN2 kinase in Drosophila's enterocytes. Our data indicate that Lp's r/tRNAs loci products activate GCN2 in a subset of larval enterocytes, a mechanism necessary for the host's adaptation to amino acid imbalance that ultimately supports growth. Our findings unravel a novel beneficial molecular dialog between hosts and microbes, which relies on a non-canonical role of GCN2 as a mediator of non-nutritional symbiotic cues encoded by r/tRNA operons.

Introduction

Nutrition is one of the major factors influencing the growth trajectory of animals (Lifshitz, 2009) and juvenile animals feeding on an inadequate source of nutrients (either in terms of nutrient quantity or quality) face important growth alteration. The gut microbiota (*i.e.* the communities of microorganisms that are found in the intestinal tract of animals) plays a major role in the interplay between nutrition and growth (Schwarzer et al., 2018) and certain strains of intestinal bacteria support the growth of animals suffering from chronic undernutrition (*i.e.* fed a nutrient-poor diet for a long period of time) (Blanton et al., 2016; Schwarzer et al., 2016). However, the mechanisms underlying the growth-supporting activities of bacterial strains during malnutrition remain largely elusive.

The fruit fly *Drosophila melanogaster* (hereinafter referred to as Drosophila) is a powerful model to study the influence of bacteria on animal growth. Indeed, Drosophila harbours simple bacterial communities, which individual components can be cultured and genetically engineered. Moreover, Drosophila's growth phase (larval stages) is short (4-5 days in optimal nutritional conditions, up to 15-20 days in severe malnutrition conditions) (Erkosar et al., 2013; Tennessen and Thummel, 2011). Chronic

undernutrition greatly delays the development of Germ-Free (GF) Drosophila larvae (*i.e.* larvae lacking a microbiota). Such delay can be buffered by the association of GF larvae with certain strains of symbiotic microbes (Gould et al., 2018; Keebaugh et al., 2018; Shin et al., 2011; Storelli et al., 2011). Several mechanisms contribute to the buffering of the effects of chronic undernutrition. First of all, symbiotic microbes can directly improve Drosophila larvae's nutrition: they can synthesize essential nutrients from other dietary nutrients and provide them to their host (Consuegra et al., 2020a; Sannino et al., 2018) or concentrate dietary nutrients, which improves their uptake by the host (Yamada et al., 2015). They can also improve nutrition indirectly: sensing of symbiotic bacteria's cell wall components by gut cells leads to the production of digestive enzymes, which helps the larva digest the dietary polypeptides and retrieve more amino acids from the diet (Erkosar et al., 2015; Matos et al., 2017). Finally, they can modulate nutrient utilization by their host. Acetate produced by symbiotic bacteria promotes growth under chronic undernutrition (Shin et al., 2011) and the underlying mechanism may rely partly on regulation of gut lipid stores; acetate alters the epigenome of enteroendocrine cells (Jugder et al., 2021), which stimulates the secretion of the hormone Tachykinin (Tk). Tk then promotes lipid utilization in nearby enterocytes, which improves larval growth (Kamareddine et al., 2018). Therefore, molecules produced by symbiotic microbes can strongly influence larval growth, whether these molecules are nutrients that directly fuel anabolic growth or non-nutrients such as cell wall components or acetate that act as signalling cues for the host, which induce physiological changes allowing adaptation to undernutrition. Beyond these few examples, we posit that symbiotic cues may be widespread in host-microbes symbiosis but their nature remains elusive. Hence, identifying them is an important goal of the field of host-symbionts interactions (Selosse et al., 2014).

Most studies on Drosophila's microbiota rely on the use of oligidic diets, *i.e.* diets made of nutritionally complex components such as inactivated yeast and cornflour. Such diets allow the experimenters to manipulate global nutrient quantity (for instance, by decreasing the amount of inactivated yeast) but not nutrient composition. Reducing the amount of inactivated yeast leads to an indiscriminate decrease of all amino acids, vitamins, lipids, cholesterol and many other unidentified compounds present in yeast cells. On the contrary, holidic diets (HD: diets made of chemically pure nutrients) allow to precisely control the nutritional composition of Drosophila's diet (Piper, 2017). Especially, the HD developed by Hinton and colleagues in the early 50' (Hinton et al., 1951) and later improved by others (Piper et al., 2014, 2017; Sang, 1956) contains all 20 proteinogenic amino acids (AA), allowing the precise control over the quantity of each AA in experimental diets. AA are among the most important nutrients for juvenile growth (Wu, 2009). AA are the building blocks of proteins, they can fuel the energy metabolism through gluconeogenesis (Grasmann et al., 2019), act as methyl donors (Niculescu and Zeisel, 2002) or as precursors for vitamins biosynthesis (Castro-Portuguez and Sutphin, 2020). The use of HD allows to create AA imbalance (keeping the total concentration of AA the same, while manipulating the respective levels of specific AA), which correspond to conditions that animals face in their natural

environment when they encounter non-optimal dietary sources. Piper and colleagues recently designed a HD which AA composition mirrors the composition of Drosophila's exome, which they called FLY AA (Piper et al., 2017). The FLY AA diet was compared to the historical MM1 AA diet (Hinton et al., 1951), which has the same overall quantity of AA and other nutrients but a different AA composition. The FLY AA diet is superior to the MM1 AA diet to support Drosophila's lifespan, fecundity and development, which indicates that AA composition in diets and not just quantity greatly influences these parameters (Piper et al., 2017).

Although AA imbalance is detrimental for several adult and juvenile traits, Eukaryotes, and in particular Drosophila, possess regulatory pathways than can sense AA imbalance and trigger physiological adaptation that mitigate its effects. The main AA (or lack of-) sensing pathways are the Target-of-Rapamycin (TOR) kinase pathway and the general control nonderepressible 2 (GCN2) kinase (Gallinetti et al., 2013). Both kinases were first described in yeast (Dever et al., 1992; Heitman et al., 1991) and orthologous pathways were found in virtually all eukaryotes, including Drosophila (Olsen et al., 1998; Zhang et al., 2002). The TOR kinase forms two protein complexes: mTORC1 and mTORC2, which can be activated by many cues (Laplante and Sabatini, 2009). Especially, mTORC1 responds to high intracellular AA levels through the action of AA transporters and AA-binding cytosolic proteins; conversely, AA scarcity represses TOR activity (Goberdhan et al., 2016). Once activated, TOR increases translation through phosphorylation of 4E-BP and S6K (Ma and Blenis, 2009). GCN2 is activated by several cues (Donnelly et al., 2013). The best-characterized cue is the quantity of uncharged tRNAs, a signature of hampered protein synthesis due to a scarcity of intracellular AA (Masson, 2019). Activation of GCN2 causes a global translational repression through phosphorylation of the Eukaryotic Initiation Factor 2 (eIF2α)(Teske et al., 2011) except for a subset of mRNAs which translation is increased, promoting adaptation to stress (Harding et al., 2003). In addition to its cell-autonomous effects, the GCN2 pathway has systemic effects in Drosophila. Ubiquitous knock-down of GCN2 in Drosophila larvae causes developmental delay (Malzer et al., 2013). Moreover, activation of GCN2 in dopaminergic neurons of the larval brain (Bjordal et al., 2014) or in the enterocytes of adult flies (Kim et al., 2021) trigger a marked behavioural response leading to the avoidance of diets with an imbalanced AA composition. In addition, GCN2 in adult enterocytes regulates gut plasticity in response to AA/sugar imbalance (Bonfini et al., 2021). Furthermore, GCN2 in the midgut or in the fat body is necessary for lifespan extension under dietary restriction (Kim et al., 2020). Finally, GCN2 in the fat body represses reproduction under AA scarcity (Armstrong et al., 2014).

Given the contribution of the microbiota in buffering Drosophila growth defects during chronic undernutrition, we wondered if and how symbiotic bacteria would buffer growth delays due to malnutrition in the form of dietary AA imbalance. In this manuscript, we found that a major Drosophila symbiont, *Lactiplantibacillus plantarum*, supports juvenile growth on AA-imbalanced diet through a mechanism that relies on the

production of ribosomal and transfer RNA by Lp, and the adaptation to AA imbalance by GCN2 activation in the enterocytes. Our study suggests that on top of its canonical role as a cellular sensor of uncharged eukaryotic tRNA, GCN2 is also a cellular mediator of symbiotic cues encoded by r/tRNA operons and supports systemic growth despite malnutrition.

Results

Association with Lp rescues amino acid imbalance

In order to first test the effect of AA imbalance on Drosophila growth independently of any microbial influence, we compared the development of GF larvae reared on the FLY AA diet, which AA composition is based on Drosophila's exome, to larvae reared on the historical MM1 AA diet (Piper et al., 2017). FLY AA and MM1 AA diets show the same total concentration of AA (10,7 $g.L^{-1}$) but differ in AA composition (Fig. 1A). GF larvae reared on the MM1 AA diet display an important growth delay compared to GF larvae reared on the FLY AA diet (Fig. 1B, grey curves). Consistently with previous observations made on larvae naturally associated with laboratory commensal microbes (Piper et al., 2017), Lp-associated larvae are slightly delayed on the MM1 AA diet compared to the FLY AA diet; however, the difference is much less important than observed for GF larvae (Fig. 1B), indicating that association with Lp rescues to a large extent the developmental delay due to AA imbalance. Flies reared on the MM1 AA diet display a decrease in fecundity compared to flies reared on the FLY AA diet, which is mainly due to the scarcity in the limiting EAA, Arginine (Arg) (Fig. 1A)(Piper et al., 2017). We observed that increasing Arg in the MM1 AA diet to reach the same level as in the FLY AA diet, while keeping the total concentration in AA stable by decreasing the concentration of the NEAA Glutamate (MM1+R^{FLY} AA, Fig. 1C) rescues the developmental delay of GF larvae (Fig. 1D). Reciprocally, decreasing Arg in the FLY AA diet to the same level as in the MM1 AA diet (~70% decrease) while keeping the total concentration in AA stable by increasing Glu concentration (FLY-R^{MM1} AA, Fig.1E) mimics the effect of the MM1 AA diet on the development of GF and Lp-associated larvae (Fig. 1F). Therefore, it seems that the phenotypical differences between FLY AA and MM1 AA is mainly caused by the low concentration of one limiting AA: Arg. It was previously shown that Drosophila's symbiotic bacteria can synthetize AA and provide them to their host to compensate for AA scarcity (Consuegra et al., 2020a; Kim et al., 2021). The fact that Lp rescues the developmental delay on MM1 AA diet and FLY-R^{MM1} AA thus suggests that Lp can provide Arg to the larva. Lp's genome encodes the enzymes necessary for Arg synthesis; however, we showed in a previous study that Lp is auxotroph to Arg and that it cannot rescue the effect of a total lack of Arg on larval development (Consuegra et al., 2020a). Therefore, we were not able to tease apart the following two hypotheses: Lp rescues the effects of Arg limitation in the MM1 AA diet by providing a small amount of Arg, or through another unrelated mechanism.

To challenge these hypotheses, we tested the effects of Lp-association on growth while limiting others EAA. We selectively decreased the concentration of each EAA by 70% from the FLY AA diet and measured the time of development of larvae (expressed as D50, *i.e.* the median time of entry into metamorphosis). As expected, decreasing the concentration of any EAA causes growth delay in GF larvae. Decreasing the amount of certain EAA (Ile, Lys, Thr, Trp, Val) completely blocks the development of GF larvae, which stall at the L2 or L3 stage. Decreasing the amount of the other EAA (Arg, His, Met, Leu, Phe) causes an important developmental delay in GF larvae compared to the FLY AA diet (Fig. 1G). In order to compare the different conditions, we aimed at finding a setup in which GF larvae are able to reach pupariation, with a strong developmental delay. We thus imposed a less severe AA imbalance by only decreasing the concentration of each EAA by 60%. We observed a similar trend: decreasing the amount of Ile, Lys, Thr, Trp or Val yields an important developmental delay in GF larvae, whereas decreasing the amount of Arg, His, Met, Leu or Phe results in a minor developmental delay (Fig. 1H). This confirms that some EAA seem to be more important than others for the development of GF larvae; alternatively, it is possible that the FLY AA diet does not contain enough of these EAA (Ile, Lys, Thr, Trp, Val) and too much of the others (Arg, His, Met, Leu, Phe).

Association with Lp rescues the effects of limitation in any EAA (Fig. 1G,H). As stated before, it is uncertain whether or not Lp can produce Arg; on the contrary, it is known that Lp's genome does not encode the enzymes necessary for the synthesis of Branched-Chained AA (BCAA: Leucine, Isoleucine and Valine) (Martino et al., 2016; Saguir and de Nadra, 2007; Teusink et al., 2005), and thus Lp cannot provide them to Drosophila (Consuegra et al., 2020a; Kim et al., 2021). Therefore, we were interested by the fact that Lp rescues the developmental delay caused by BCAA limitation, which it cannot synthetize *de novo*. We thus decided to focus on diets limited in Valine (Val) to decipher the mechanisms underlying such beneficial effect of Lp on its host growth. We thereafter refer to the FLY AA diet as "balanced diet", and to the FLY AA -60% Val diet as "imbalanced diet". Decreasing Val by 60% results in a strong delay in the growth of GF larvae, which is almost completely rescued by association with Lp (Fig. 1I). Replacing the missing Val with an equal quantity of another EAA (Leu or His) does not improve the development of GF larvae (Fig. 1J). This further shows that the delay observed on imbalanced diet is due to AA imbalance rather than total AA scarcity. Of note, further decreasing Val concentration (-80%, -90%) is lethal to GF larvae, but not to Lp-associated larvae (Fig. S1A). Completely removing Val from the diet is lethal to both GF larvae and Lp-associated larvae (Consuegra et al., 2020a). On the contrary, increasing Val by 100% compared to its initial levels does not impact the development of GF or Lp-associated larvae (Fig. S1B). Moreover, egg-to-pupa survival is not impacted by AA imbalance nor by association with Lp (Fig. S1C). Finally, supplementing the GF larvae with Heat-Killed (HK) Lp does not rescue the effects of an imbalanced diet on larval growth, which shows that the Val brought by the inoculation of Lp at the beginning of the experiment is not sufficient to restore Val levels required for larval growth (Fig. S1D). Taken together, these results demonstrate that

Lp can rescue the effects of AA imbalance due to a single dietary EAA limitation on larval growth through a mechanism independent of AA providing. Instead, we posit that Lp promotes adaptation of its host's physiology to AA imbalance to support larval growth.

Figure 1

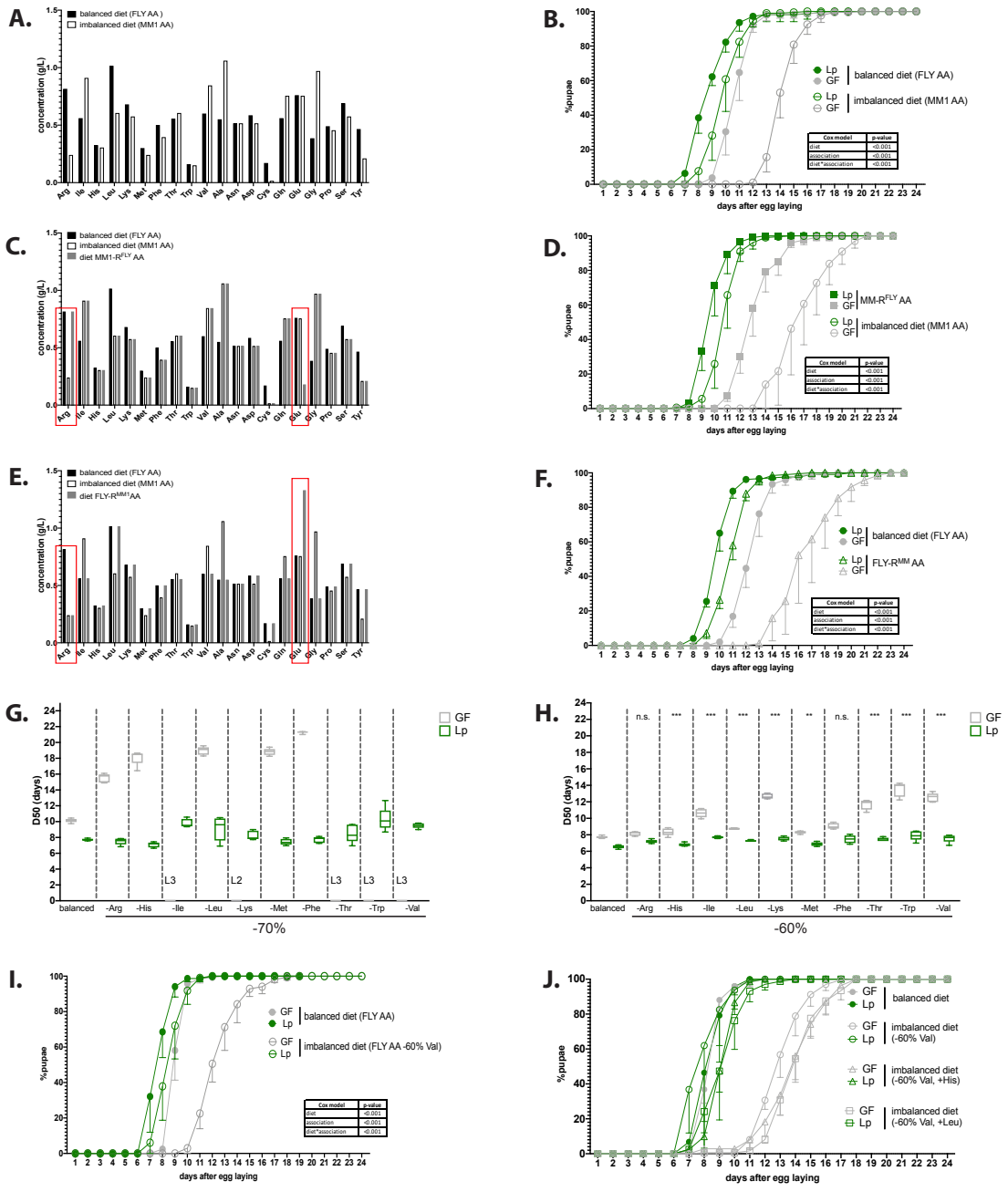

Fig. 1 Lp rescues the developmental delay due to AA imbalance.
(A,C,E) AA composition of the diets. The Y-axis represents the concentration of each AA ($g.L^{-1}$). **(B, D, F, I, J)** Developmental timing of larvae raised on holidic diets in GF condition (grey) or Lp-associated condition (green). The graphs represent the total fraction of emerged pupae over time as a percentage of the final number of pupae. When indicated, we used a Cox proportional hazards model to test the effect of the diet, the association with Lp, and the interaction between these two parameters. **(A)** AA

composition of the balanced diet (FLY AA, black bars) and the imbalanced diet (MM1 AA, white bars). **(B)** Developmental timing of larvae raised on balanced diet (FLY AA, filled circles) or imbalanced diet (MM1 AA, empty circles) **(C)** AA composition of the balanced diet (FLY AA, black bars), the imbalanced diet (MM1 AA, white bars) and the diet MM1-R^{FLY} AA (grey bars), which composition is the same as MM1 AA except for Arg (same concentration as in FLY AA) and Glu (decreased to keep total AA concentration stable) as shown by the red squares. **(D)** Developmental timing of larvae raised on imbalanced diet (MM1 AA, empty circles) or MM1-R^{FLY} AA diet (filled squares). **(E)** AA composition of the balanced diet (FLY AA, black bars), the imbalanced diet (MM1 AA, white bars) and the diet FLY-R^{MM1} AA (grey bars), which composition is the same as FLY AA except for Arg (same concentration as in MM1 AA) and Glu (increased to keep total AA concentration stable) as shown by the red squares. **(F)** Developmental timing of larvae raised on balanced diet (FLY AA, filled circles) or FLY-R^{MM1} AA diet (empty triangles). **(G,H)** Developmental timing of GF larvae (grey) and Lp-associated larvae (green) on FLY AA diets with a -70% **(G)** or -60% **(H)** decrease in each EAA. Boxplots show maximum, minimum and median D50 (median time of pupariation) of each replicate. L2: larvae stalled at the L2 stage. L3: larvae stalled at the L3 stage. For each diet in **(H)**, we used a Cox proportional hazards model to test the effect of the diet, association with Lp, and the interaction between these two parameters. We show the p-values of the interactions between diet and association with Lp after correction by the FDR method. n.s.: non-significant, **: p-value<0.01, ***: p-value<0.001. **(I)** Developmental timing of larvae raised on balanced diet (FLY AA, filled circles) or imbalanced diet (FLY AA-60% Val, empty circles). **(J)** Developmental timing of larvae raised on balanced diet (FLY AA, filled circles), on imbalanced diet (FLY AA Val-60%, empty circles), on imbalanced diet adjusted with His (FLY AA Val -60% + His, triangles) or on imbalanced diet adjusted with Leu (FLY AA Val -60% + Leu, squares).

Figure S1

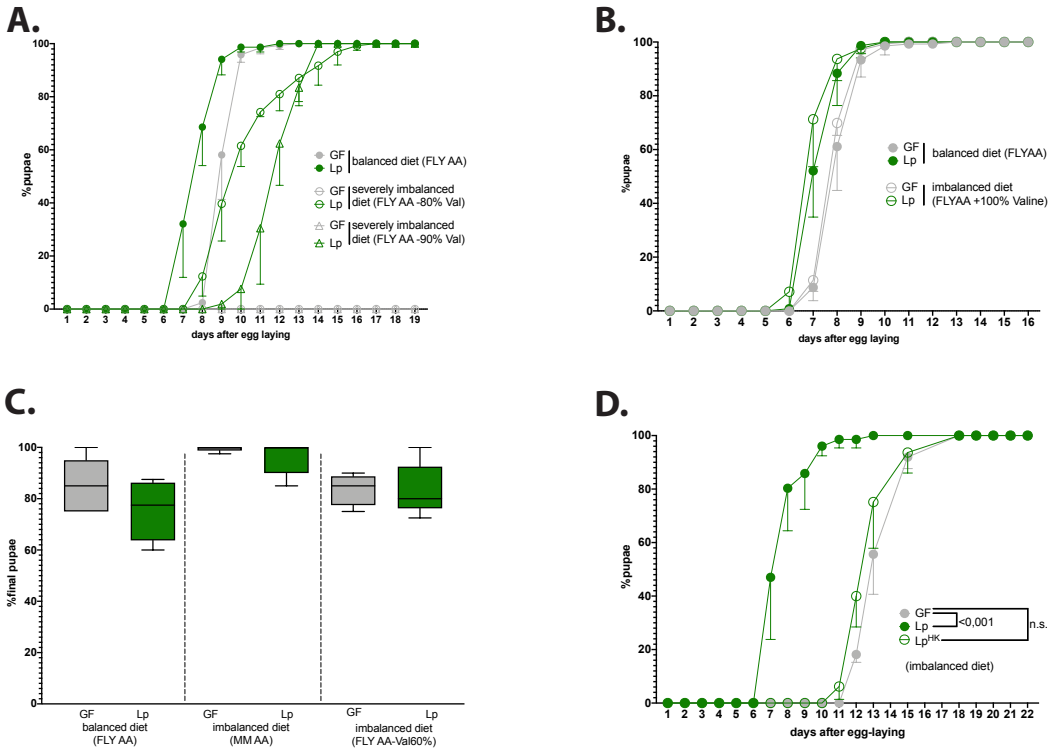

Fig. S1

(A) Developmental timing of larvae raised on balanced diet (FLY AA, filled circles) or on severely imbalanced diets (FLY AA -80% Val, empty circles, FLY AA -90% Val, empty triangles) in GF condition (grey) or Lp-associated conditions (green). The graph represents the total fraction of emerged pupae

over time as a percentage of the final number of pupae. GF larvae reared on severely imbalanced diets (-80% or -90% Val) did not reach pupariation. **(B)** Developmental timing of larvae raised on balanced diet (FLY AA, filled circles) or on imbalanced diet due to excess Val (FLY AA +60% Val, empty circles). **(C)** Egg-to-pupa survival of GF larvae (in grey) and Lp-associated larvae (green) on balanced diet and imbalanced diets. Survival was calculated as the final number of pupae divided by the initial number of eggs (*i.e.* 40 per replicate). We performed a Kruskal-Wallis test followed by post-hoc Dunn's tests to compare each condition to the condition GF on balanced diet and found no statistically significant difference. **(D)** Developmental timing of larvae raised on imbalanced diet (FLY AA Val -60%) in GF conditions (grey), in Lp-associated conditions (filled green circles) or after supplementation with the same quantity of Heat-Killed (HK) Lp (empty green circles). We used a Cox proportional hazards model to compare the effect of Lp and HK Lp to the GF condition.

Rescue of AA imbalance by Lp requires r/tRNAs operons in Lp

In order to decipher how Lp rescues the effects of AA imbalance on host growth, we performed a genetic screen using a transposon insertion library of Lp (Fig. 2A). This library is composed of 2091 mutants, each carrying a transposon randomly inserted in the chromosome, including 1218 insertions inside open reading frames (Matos et al., 2017). We mono-associated GF larvae with each mutant of the library and looked for transposon insertions in Lp's genome altering the capacity of Lp to support larval development on a severely imbalanced diet (FLY AA -80%Val, Fig. S1A). For each mutant, we calculated the D50 (median time of entry into metamorphosis) and normalized it into a z-score. We applied a threshold of z-score>2.5 and identified 32 insertional mutants. Association with these mutants thus results in a delayed time of larval development on a severely imbalanced diet (Fig. 2B). To validate these 32 candidates, we individually re-tested them in multiple (5) replicates. We compared the development of larvae associated with the 32 candidates to larvae associated with an intergenic region insertion strain showing a WT-like phenotype (mutant B02.04, z-score=0.65). Thus, we discarded 23 false positives and retained only 9 candidates which result in a significant and robust developmental delay on an imbalanced diet upon association (Fig. 2C).

Upon fly larvae association Lp grows on the fly food and constantly and repetitively transits through the larval gut (Storelli et al., 2018). The quantity of live bacteria present in the food can greatly impact the growth-promoting capacity of Lp (Consuegra et al., 2020b; Keebaugh et al., 2018). As a consequence, a Lp strain that grows poorly on the food matrix would not support larval growth. Since we wanted to exclude such candidates, we tested the growth of the 9 candidates on imbalanced HD, in the presence of larvae (Fig. 2D). 3 candidates (B08.06, F09.11 and H04.06) show growth defects and thus were not retained for further analysis. On the contrary, the remaining 6 candidates (B12.11, C08.20, C09.09, D12.09, D12.16, F07.08) show no growth defect. Moreover, they do not show any impairment at colonizing the larval gut (Fig. 2E). For further characterization, we tested whether the effect of the mutations may also be observed on a moderately imbalanced diet (-60% Val). On such diet, the mutations B12.11 and C08.20 do not significantly impact Lp's ability to rescue the

developmental delays of larvae. On the contrary, larvae associated with the mutants C09.09, D12.09, D12.16 and F07.08 are still delayed compared to the larvae associated with the WT-like mutant B02.04 (Fig. 2F), though the difference is less important than on a severely imbalanced diet (-80% Val, Fig. 2C).

Next, we sequenced the genomes of the 6 selected candidates to determine in which genomic regions the transposons were inserted. Interestingly, 4 out of the 6 candidates (mutants C09.09, D12.09, D12.16 and F07.08) showed independent transposon insertions in operons containing genes encoding transfer RNAs (tRNAs) and/or ribosomal RNAs (rRNA) (Fig. 2G). These four mutants are also the ones that seem to most affect larval development on imbalanced diet (Fig. 2F). C09.09 and F07.08 display independent insertions in the same operon, but at different loci (upstream the 16S rRNA for C09.09 and inside the 23S rRNA for F07.08, Fig. 2G).

To confirm the importance of r/tRNA operons in supporting larval growth, we generated a deletion mutant of the whole operon identified in the insertion mutants C09.09 and F07.08 ($\Delta op_{r/tRNA}$) by homology-based recombination (Matos et al., 2017). $\Delta op_{r/tRNA}$ shows the same phenotype as the insertion mutants in terms of lack of rescue of AA imbalance (Fig. S2A), growth on imbalanced HD in the presence of larvae (Fig. S2B) and larval gut colonization (Fig. S2C). Of note, the chromosome of Lp contains five operons encoding r/tRNAs, which may explain why deleting one of such operons does not have a major impact on bacterial fitness. However, it seems that the production of r/tRNAs (or any other yet unknown product of this loci) from these operons is necessary to the rescue of the delay due to AA imbalance by Lp.

Figure 2

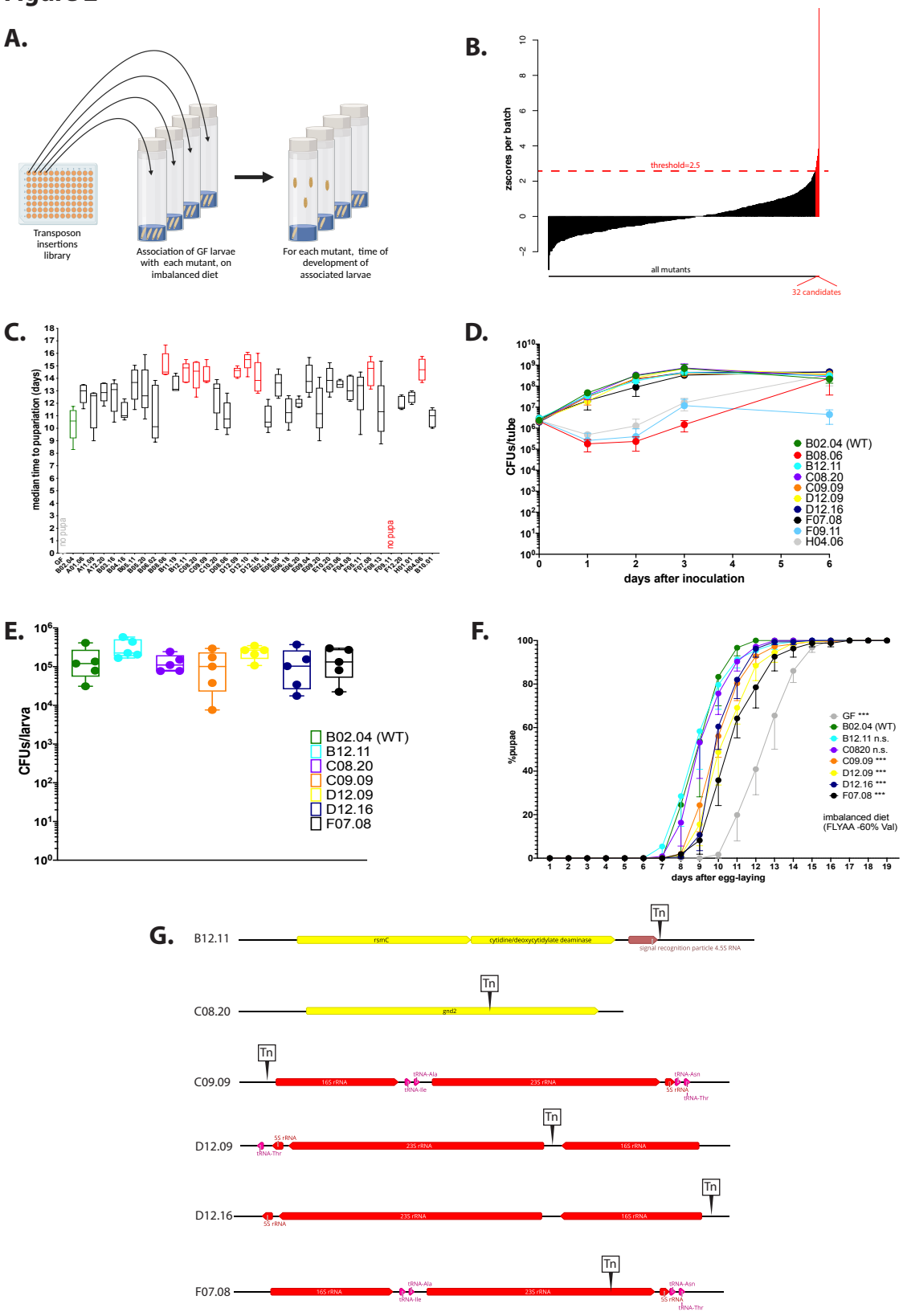

Fig. 2 The operons encoding ribosomal and transfer RNAs in Lp are necessary for Lp to rescue the delay due to AA imbalance.

335 **(A)** Representation of the genetic screen. **(B)** Result of the screen: for each mutant (X-axis), we calculated the median time of development of associated larvae and normalized it into a z-score (Y-

axis). We selected the 32 candidates that yielded a z-score>2.5. **(C)** Developmental timing of GF larvae (grey) and larvae associated with WT-like mutant B02.04 (green) or the 32 candidate mutants from the genetic screen, on a severely imbalanced diet (FLY AA -80% Val). GF larvae and larvae associated with mutant F09.11 did not reach pupariation. Boxplots show maximum, minimum and median of D50 (median time of pupariation) of each replicate. We performed a Kruskal-Wallis test followed by post-hoc Dunn's tests to compare all mutants to B02.04. In red: statistically significant difference with B02.04 (p-value<0.05). **(D)** Growth of the 9 candidates on imbalanced diet (FLY AA -60% Val), in association with larvae. The graph shows the quantity of Colony-Forming Units (CFUs) of Lp over time. **(E)** Colonization of the larval gut by the 6 remaining candidates, on imbalanced diet (FLY AA -60% Val). The graph shows the quantity of Colony-Forming Units (CFUs) of Lp per larva. We performed a Kruskal-Wallis test followed by post-hoc Dunn's tests to compare each candidate to B02.04 and found no statistically significant difference. **(F)** Developmental timing of larvae raised on imbalanced diet (FLY AA-60% Val), in GF condition or in association with each one of the six candidates or with B02.04. The graph represents the total fraction of emerged pupae over time as a percentage of the final number of pupae. We used a Cox proportional hazards model to compare the effect of each candidate to the effect of B02.04. The p-values were adjusted by the Tukey method. n.s.: non-significant. ***: p-value<0.001. **(G)** Representation of the six transposon insertions. Tn: transposon. rspC: 16S rRNA methyltransferase. gnd2: phosphogluconate dehydrogenase. Of note, C09.09 and F07.08 show two independent insertions in the same r/tRNA operon.

Fig. S2

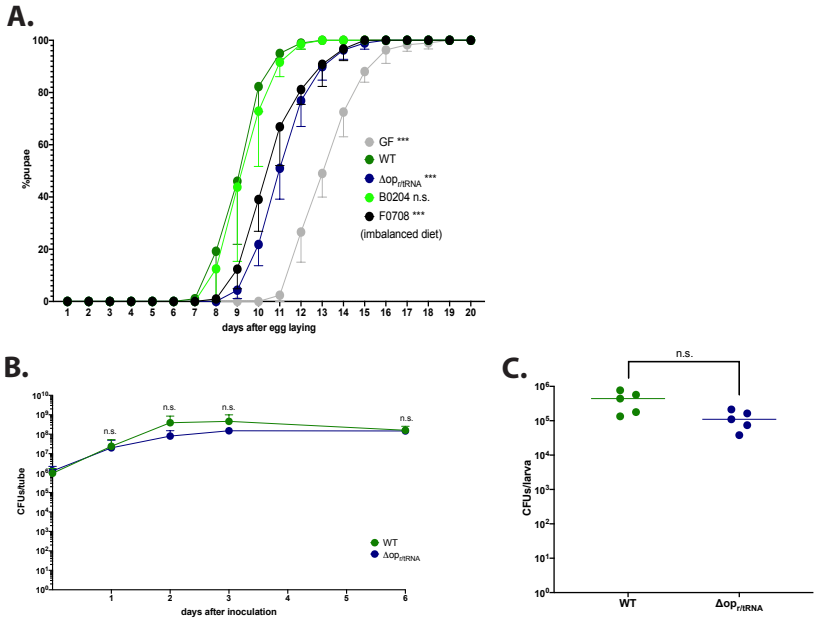

Fig. S2

(A) Developmental timing of larvae raised on imbalanced diet (FLY AA-60% Val), in GF condition or in association with Lp (dark green), WT-like mutant B02.04 (light green), Lp $\Delta op_{r/tRNA}$ (dark blue) or r/tRNA insertion mutant F07.08 (black). The graph represents the total fraction of emerged pupae over time as a percentage of the final number of pupae. We used a Cox proportional hazards model to compare the effect of each candidate to the effect of Lp. The p-values were adjusted by the Tukey method. n.s.: non-significant. ***: p-value<0.001. **(B)** Growth of Lp (dark green) and Lp $\Delta op_{r/tRNA}$ (dark blue) on imbalanced diet (FLY AA -60% Val), in association with larvae. The graph shows the quantity of Colony-Forming Units (CFUs) of Lp over time. We performed a Mann-Whitney test at each time point and found no

statistically significant difference. **(C)** Colonization of the larva gut by Lp (dark green) and Lp $\Delta op_{r/tRNA}$ (dark blue) on imbalanced diet (FLY AA -60% Val). The graph shows the quantity of Colony-Forming Units (CFUs) of Lp per larva. We performed a Mann-Whitney test and found no statistically significant difference.

Lp activates GCN2 signalling in the anterior midgut

Small RNA from bacteria can be sensed by eukaryotic host's cells and modulate host's immune signalling (Koeppen et al., 2016; Moriano-Gutierrez et al., 2020; Ren et al., 2019). We hypothesized that products of the r/tRNAs loci may be microbial cues sensed by host cells to promote physiological adaptation. The general control nonderepressible 2 (GCN2) kinase can bind unloaded tRNAs (Wek et al., 1995) and rRNAs (Zhu and Wek, 1998). Moreover, the GCN2 pathway is one of the main pathways that allow eukaryotic cells to adapt to AA imbalance (Gallinetti et al., 2013). Finally, GCN2 is active in Drosophila's gut (Bonfini et al., 2021; Kim et al., 2021), where Lp is in close proximity to its host's cells (Fig. S3A). Therefore, we wondered if GCN2 may be a sensor and signalling intermediary between r/tRNA from Lp and host physiological adaptation to an imbalanced diet.

We first tested whether Lp association regulates GCN2 activation in the larval gut. In Drosophila, the transcription factor ATF4 acts downstream of GCN2 and binds to recognition sites in the first intron of the gene *4E-BP* (*Thor* in Drosophila) to activate its transcription (Kang et al., 2017). Kang and colleagues previously generated a transgenic line (4E-BP^{intron}dsRed), which carries a fluorophore under the transcriptional control of the first intron of *4E-BP*. This reporter thus allows to visualize the pattern of activity of ATF4 downstream of GCN2 activation (Kang et al., 2017; Vasudevan et al., 2017). We used the 4E-BP^{intron}dsRed reporter as a molecular readout to probe GCN2 activity in the larval midgut in response to Lp association. Fig. S3B shows the pattern of expression of the 4E-BP^{intron}dsRed reporter in dissected guts of larvae fed an imbalanced diet (top panel) or a balanced diet (bottom panel), either GF (left panel) or Lp-associated (right panel). Similarly to what was previously reported (Kang et al., 2017), we observed 4E-BP^{intron}dsRed reporter expression in the gastric caeca, the proventriculus and in the middle midgut, in a region known as the acidic zone (Overend et al., 2016). This pattern is conserved between GF larvae and Lp-associated larvae. Conversely, the 4E-BP^{intron}dsRed reporter is expressed in the anterior midgut specifically in Lp-associated larvae, while this signal is absent from GF guts (Fig. S3B, red squares and Fig. 3A). We confirmed by RT-qPCR that endogenous GCN2-dependant *4E-BP* expression is induced in the anterior midgut upon Lp-association on an imbalanced diet (Fig. S3C). Interestingly, expression of the 4E-BP^{intron}dsRed reporter in this region depends on the association with Lp, but not on AA imbalance as we observed it in larvae raised on either imbalanced diet (Fig. 3A, top panel) or balanced diet (Fig. 3A, bottom panel; quantification of the signal is shown in

Fig. 3B). Lp can thus activate the 4E-BP^{intron}dsRed reporter specifically in the anterior midgut, independently of dietary AA imbalance.

ATF4 is activated by eIF2α, which can be phosphorylated by GCN2 but also by other kinases such as PERK (Teske et al., 2011). In order to test whether the 4E-BP^{intron}dsRed reporter indeed mirrors GCN2 activity, we looked at its pattern of expression in a GCN2 knock-down background. Inhibition of GCN2 expression using tissue specific *in vivo* RNAi (Dietzl et al., 2007) completely abrogates the activation of the 4E-BP^{intron}dsRed reporter by Lp in the anterior midgut of larvae reared on imbalanced diet (Fig. 3C,D) or balanced diet (Fig. 3E,F). Therefore, our results establish that Lp promotes GCN2 activity in the anterior midgut of larvae, independently of AA imbalance.

Figure 3

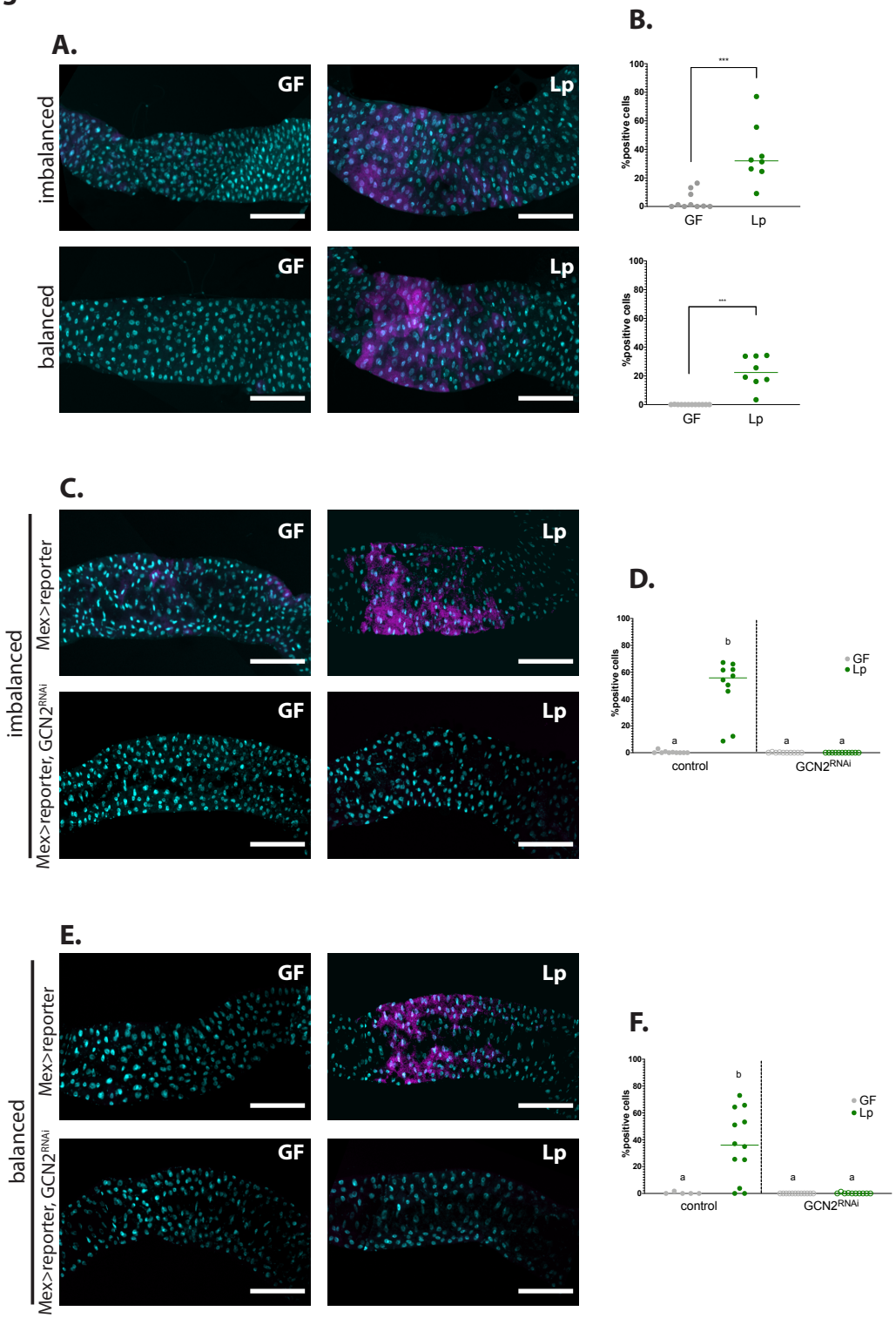

Fig. 3 Association with Lp activates GCN2 in the larval anterior midgut.
(A,C,E) Representative pictures of the anterior midgut of 4E-BP^{intron}dsRed larvae. Cyan: DAPI. Magenta: 4E-BP^{intron}dsRed reporter. Scale bar: 200 µm. **(B,D,F)** Quantification of the signal: proportion of enterocytes positive for 4E-BP^{intron}dsRed reporter's activity in the anterior midgut. Each dot represents an independent replicate. The bar shows the mean. **(A)** Larvae in GF conditions (left) or Lp-associated conditions (right) on imbalanced (FLY AA -60% Val, top) or balanced (FLY AA, bottom) diet. Quantification of the signal in **(B)**: GF larvae (grey) or Lp-associated larvae (green) fed an imbalanced

(top) or balanced (bottom) diet. We performed a Mann-Whitney test to compare the GF and Lp-associated conditions. **: p-value<0.01. ***: p-value<0.001. **(C-E)** Control larvae (Mex-Gal4 x 4E-BP^{intron}dsRed reporter) (top panel) and GCN2 knock-down (Mex-Gal4 x 4E-BP^{intron}dsRed reporter, UAS-GCN2^{RNAi}) (bottom panel) in GF conditions (left) and Lp-associated conditions (right) fed an imbalanced diet (FLY AA -60% Val) **(C)** or a balanced diet **(E)**. Quantification of the signal in **(D,F)**: GF larvae (grey circles) or Lp-associated larvae (green circles) fed an imbalanced diet **(D)** or a balanced diet **(F)**. Filled circles: control condition (Mex-Gal4 x 4E-BP^{intron}dsRed reporter). Empty circles: GCN2 knock-down (Mex-Gal4 x 4E-BP^{intron}dsRed reporter, UAS-GCN2^{RNAi}). We performed a Kruskal-Wallis test followed by post-hoc Dunn's tests to compare all conditions together. a: the conditions are not significantly different from each other (p-value>0.05). b: the condition is significantly different from other conditions (p-value<0.01).

Figure S3

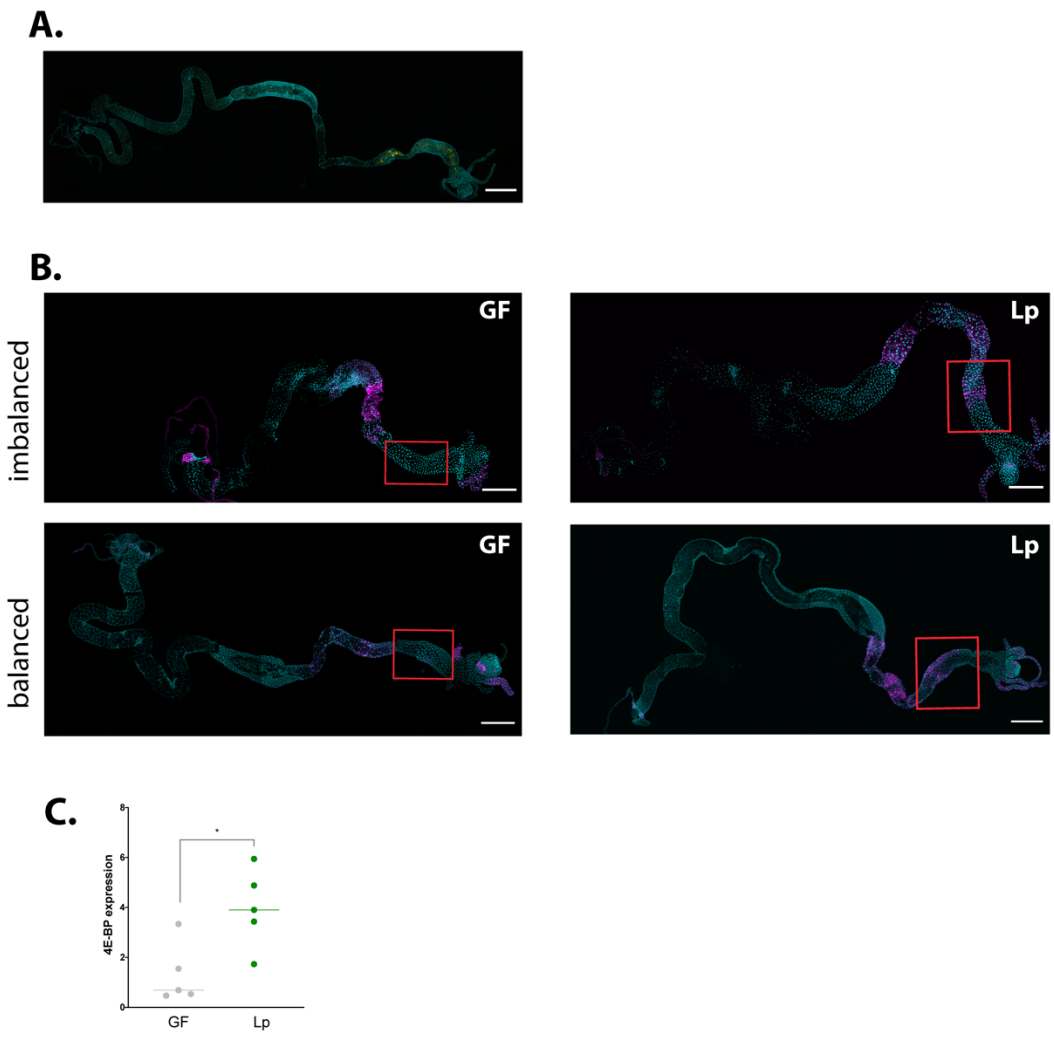

Fig. S3

(A) Representative picture of the full gut of a larva associated with Lp^{GFP}. Cyan: DAPI. Yellow: GFP. Scale bar: 500 µm. **(B)** Representative pictures of the full gut of a GF larva (left panel) and a Lp-associated larva (right panel) fed an imbalanced diet (FLY AA -60% Val, top panel) or a balanced diet (FLY AA, bottom panel). Cyan: DAPI. Magenta: 4E-BP^{intron}dsRed reporter. The red squares show the region of the anterior midgut where Lp activates the 4E-BP^{intron}dsRed reporter. Scale bar: 500 µm. **(C)**

4E-BP expression in the anterior midgut of larvae reared on imbalanced diet (FLY AA -60% Val) in GF conditions (grey) or Lp-associated conditions (green). Expression is normalized with the expression of *rp49* using the formula $2^{Cq(rp49)-Cq(4E\text{-}BP)}$. We performed a Mann-Whitney test to compare the two conditions. *: p-value<0.05.

Lp mutants for r/tRNA operon fail to activate GCN2 in the anterior midgut

We then tested whether activation of GCN2 by Lp depends on its r/tRNA loci. To this end, we compared the induction of the 4E-BP^{intron}dsRed reporter in larvae associated with r/tRNA insertion mutant F07.08 and in larvae associated with WT-like insertion mutant B02.04. On an imbalanced diet, F07.08-associated larvae show a reduced activation of GCN2 compared to B02.04-associated larvae, though the difference is not statistically significant (Fig. 4A,B). On a balanced diet, GCN2 activation in F07.08-associated larvae is clearly altered: it is comparable to GCN2 activation in GF larvae, and significantly different from GCN2 activation in control B02.04-associated larvae (Fig. 4C,D). Similarly, we observed that association with $\Delta op_{r/tRNA}$ yields a reduction of GCN2 activation comparable to what we observed with F07.08 (on imbalanced diet: Fig. S4A,B; on balanced diet: Fig. S4C,D). The lesser difference observed on imbalanced diet might be due to longer association of the larvae with F07.08: indeed, in order to size-match the larvae, we collect them 24h before the emergence of the first pupae, which is D6 after egg-laying for B02.04 and D8 after egg-laying for F07.08. To ensure comparable association time with the two mutants, we thus performed short-term association of GF larvae with B02.04 or F07.08: the larvae were reared GF, associated with B02.04 or F07.08 at D8 after egg-laying, and collected for dissection at D10 after egg-laying. In short-term association on an imbalanced diet, activation of GCN2 is significantly reduced in F07.08-associated larvae compared to B02.04-associated larvae (Fig. 4E,F).

Uncharged tRNAs and rRNA from eukaryotic cells are canonical activators of GCN2 kinase (Masson, 2019; Zhu and Wek, 1998). It is currently unknown whether bacterial r/tRNAs can activate GCN2 as well. We therefore tested this hypothesis by feeding purified bacterial tRNAs to GF larvae carrying the 4E-BP^{intron}dsRed reporter. At the highest dose tested (625 µg), bacterial tRNAs significantly increase the expression of the reporter in the anterior midgut (Fig. S4E). This increase is comparable to the effect of feeding eukaryotic tRNAs to these larvae, though slightly inferior. However, the effect is minimal as compared to the association of larvae with Lp (Fig. S4F). Of note, Lp reaches a maximum of ~$2.5x10^9$ CFUs.mL^{-1} in HD (Fig. 2D). Based on observations made on other bacteria, this may yield ~225 µg of tRNAs in a 10 mL vial (Battley, 1988). This value is probably an underestimate, because tRNAs may accumulate during the stationary phase of Lp; the value of 625 µg thus appears to be in the physiological range of larvae's exposure. These results therefore suggest that Lp's tRNA may be direct activators of GCN2 in enterocytes. However, we cannot exclude that Lp's rRNAs, or other yet unknown products of this loci or an indirect mechanism dependent on a functional Lp r/tRNA operon is at play.

Figure 4

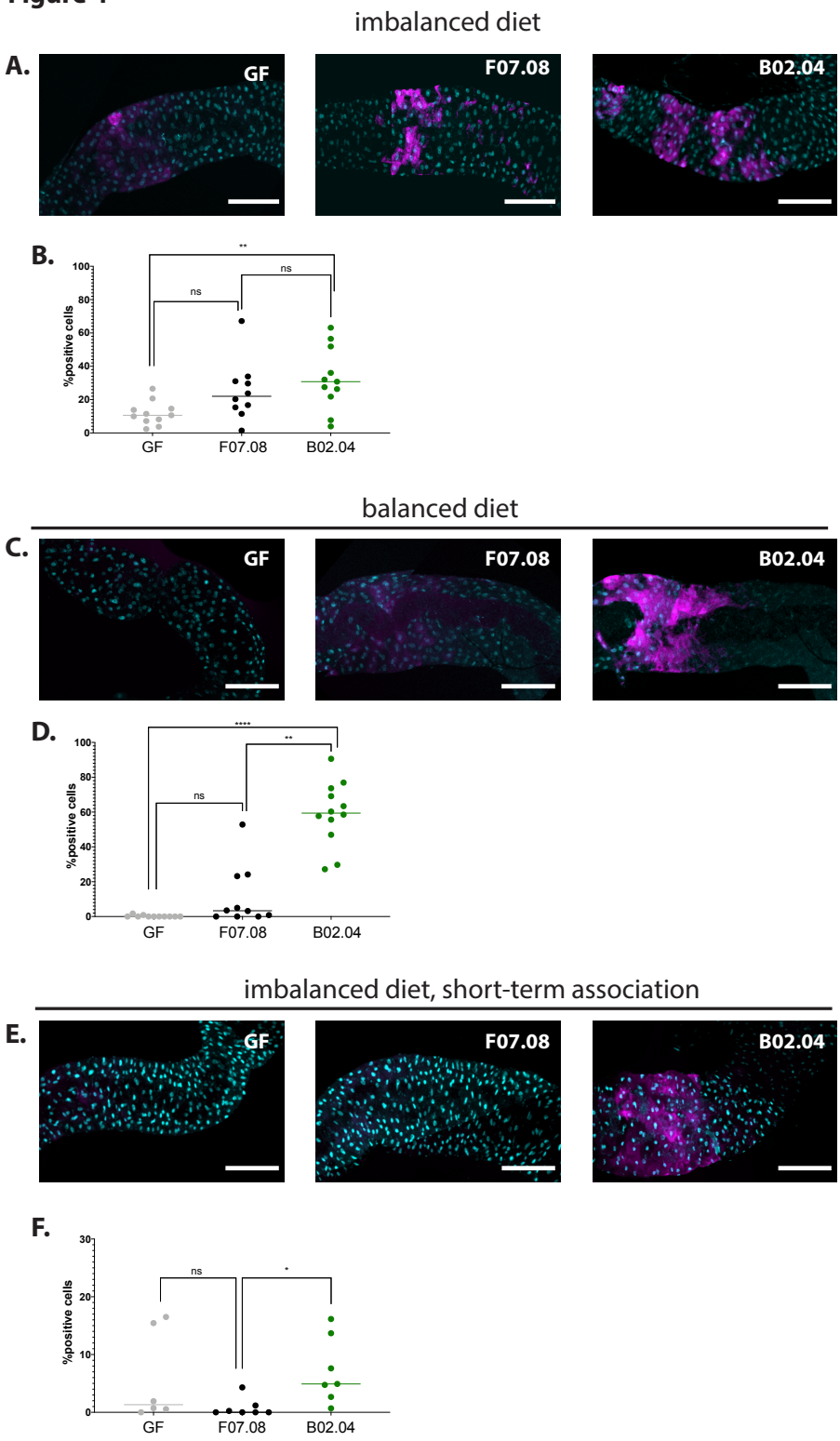

Fig. 4 Lp mutants for r/tRNA operon fail to activate GCN2 in the anterior midgut

500 **(A,C,E)** Representative pictures of the anterior midgut of 4E-BP^{intron}dsRed larvae in GF conditions (left panels), in association with r/tRNA mutant F07.08 (middle panels) or in association with WT-like mutant B02.04 (right panels). Cyan: DAPI. Magenta: 4E-BP^{intron}dsRed reporter. Scale bar: 200 µm. **(B,D,F)** Quantification of the signal: proportion of enterocytes positive for 4E-BP^{intron}dsRed reporter's activity in the anterior midgut of GF larvae (grey), larvae associated with F07.08 (black) and larvae associated

with B02.04 (black). Each dot represents an independent replicate. The bar shows the mean. We performed a Kruskal-Wallis test followed by post-hoc Dunn's tests to compare the conditions together. n.s.: non-significant. *: p-value<0.05. **: p-value<0;01. **(A)** Larvae fed an imbalanced diet (FLY AA -60% Val), signal quantified in **(B)**. **(C)** Larvae fed a balanced diet (FLY AA), signal quantified in **(D)**. **(E)** Larvae fed an imbalanced diet (FLY AA -60% Val) upon short-term association with Lp, signal quantified in **(F)**.

Figure S4

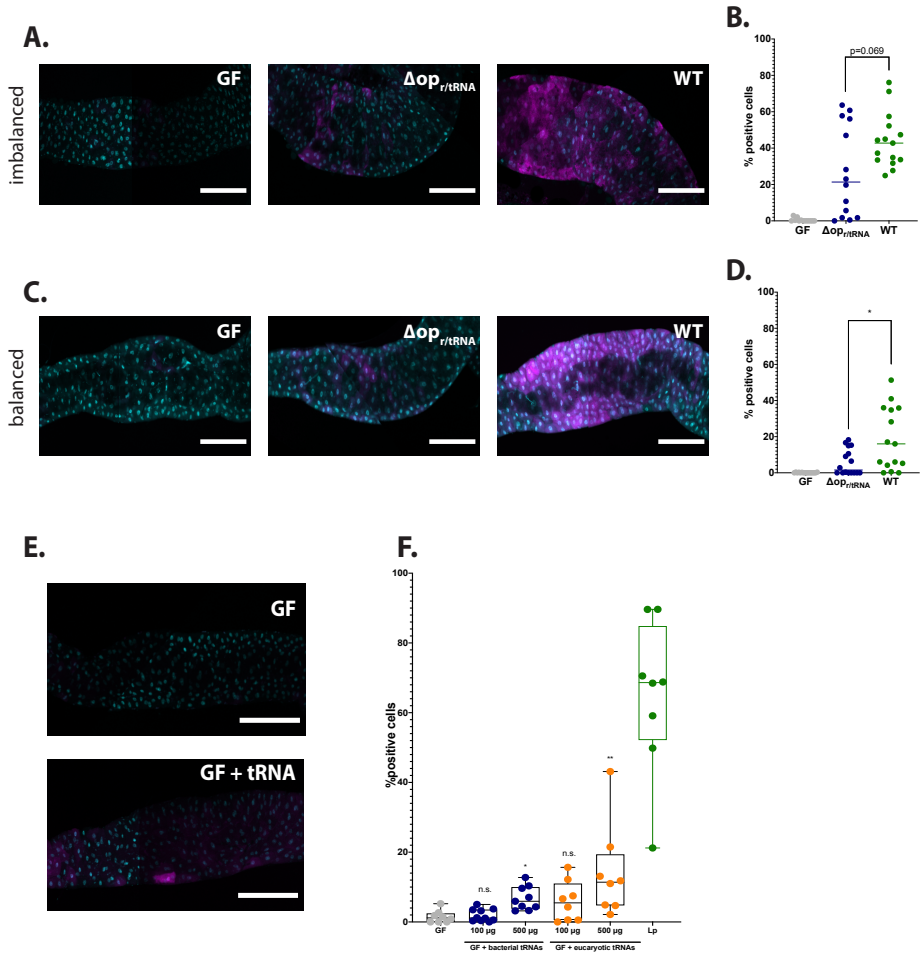

Fig. S4

(A,C) Representative pictures of the anterior midgut of 4E-BP^{intron}dsRed larvae in GF conditions (left panels), in association with Lp Δop$_{r/tRNA}$ (middle panels) or in association with Lp (right panels). Cyan: DAPI. Magenta: 4E-BP^{intron}dsRed reporter. Scale bar: 200 µm. **(B,D)** Quantification of the signal: proportion of enterocytes positive for 4E-BP^{intron}dsRed reporter's activity in the anterior midgut of GF larvae (grey), larvae associated with Lp Δop$_{r/tRNA}$ (blue) and larvae associated with Lp (green). Each dot represents an independent replicate. The bar shows the mean. We performed Mann-Whitney test to compare association with Lp and association with Lp Δop$_{r/tRNA}$. *: p-value<0.05. **(A)** Larvae fed an imbalanced diet (FLY AA -60% Val), signal quantified in **(B)**. **(C)** Larvae fed a balanced diet (FLY AA), signal quantified in **(D)**. **(E)** Representative images of 4E-BP^{intron}dsRed GF larvae (top panel) and 4E-BP^{intron}dsRed GF larvae fed 625 µg of bacterial tRNAs (bottom panel) on balanced diet (FLY AA). Cyan: DAPI. Magenta: 4E-BP^{intron}dsRed reporter. **(F)** Quantification of the signal: proportion of enterocytes positive for 4E-BP^{intron}dsRed reporter's activity in the anterior midgut of GF larvae (grey), GF larvae fed

with increasing concentrations of bacterial tRNAs (blue) or yeast tRNAs (orange) and Lp-associated larvae (green) on balanced diet (FLY AA). We performed a Kruskal-Wallis test followed by post-hoc Dunn's tests to compare each condition to GF. n.s.: non-significant. *: p-value<0.05. **: p-value<0.01. ***: p-value<0.001.

Rescue of AA imbalance by Lp requires GCN2 in the larval midgut

Therefore, association with Lp activates GCN2 in the anterior midgut of larvae in a r/tRNA loci-dependent manner. We thus sought to test whether GCN2 activation in enterocytes is necessary for Lp to rescue the developmental delay due to AA imbalance. To this end, we specifically knock-downed GCN2 in enterocytes and followed the developmental timing of GF or Lp-associated larvae in AA-imbalanced conditions. On an imbalanced diet (-60% Val), GCN2 knock-down in enterocytes causes a significant developmental delay in Lp-associated larvae compared to control larvae (Fig. 5A), a phenotype that we confirmed by using two other GCN2 RNAi lines (Fig. S5A,B) and by measuring the efficacy of RNA interference against GCN2 expression in the midgut (Fig. S5C). Of note, GCN2 knock-down in enterocytes does not alter colonization of the gut by Lp (Fig. S5D). Knocking-down GCN2 in the gut has no effect on larvae developing on an AA-balanced diet (Fig. 5B). Taken together, our results indicate that GCN2 is necessary for Lp to rescue the developmental delay due to Val limitation. We wondered whether GCN2 is necessary to rescue AA imbalance due to limitation in other AAs. We decreased the amount of each EAA identified in Fig. 1H as most important for GF larvae (Ile, Lys, Thr and Trp) by 60% and measured the growth of larvae knocked-down for GCN2. We found that GCN2 is necessary for Lp to rescue the scarcity in Ile or Thr, but not in Trp or Lys (Fig. 5C-F). Lp can synthesize Lys and Trp, but not Ile (Consuegra et al., 2020a); therefore, it seems that GCN2 is necessary only when the limiting AA cannot be provided by Lp. Lp can produce Thr, but in limiting quantity (Consuegra et al., 2020a), which may explain why GCN2 is also necessary for Lp to rescue the delay due to Thr scarcity.

Lab-reared Drosophila are mostly associated with bacteria belonging to the families *Lactobacillales* and *Acetobacteraceae* (Staubach et al., 2013). We tested whether a representative *Acetobacteraceae* strain, *Acetobacter pomorum*^{WJL} (Ap) that promotes larval growth on oligidic nutrient-poor diet (Shin et al., 2011) and on holidic diet (Consuegra et al., 2020b) displays the same properties as Lp. Ap rescues the developmental delay due to AA imbalance to the same extent as Lp (Fig. S6A). However, conversely to Lp, Ap's support to larval development upon Val limitation is independent of GCN2 expression in the gut (Fig. S6B). This is likely explained by the ability of Ap to produce Val and rescue the host's auxotrophy to Val (Consuegra et al., 2020a). Interestingly, Ap does not activate GCN2 in the anterior midgut of larvae on imbalanced diet (Fig. S6C,D) or balanced diet (Fig. S6E,F). Therefore, the ability to activate GCN2 in the anterior midgut is not common to all symbiotic bacteria and a specific attribute of Lp-mediated benefit.

In Drosophila, it was previously reported that AA scarcity engages the GCN2 pathway in enterocytes of the midgut (Bonfini et al., 2021; Kim et al., 2021) but also in brain dopaminergic neurons (Bjordal et al., 2014) and in fat body cells (Armstrong et al., 2014). Given that GCN2 activity in dopaminergic neurons of the larval brain promotes avoidance to EAA-deficient diets (Bjordal et al., 2014), we tested whether association with Lp alters larval food intake in our experimental conditions where larvae have no food choice to operate. We observed that Lp association does not alter food intake on imbalanced (Fig. S5E) or balanced diets (Fig. S5F). Moreover, knocking-down GCN2 expression in fat body cells has no impact on the development of Lp-associated larvae fed an imbalanced diet (Fig. S5G). These results suggest that the phenotype that we observe engages GCN2 in enterocytes, rather than in other tissues. Of note, although the target-of-rapamycin (TOR) pathway is another major factor supporting systemic host growth in the fat body (Colombani et al., 2003) and in enterocytes (Redhai et al., 2020), it is not required in the fat body nor in enterocytes for Lp to rescue AA imbalance. However, it is important to support the growth of GF animals (Fig. S5H,I).

Upon activation, GCN2 phosphorylates eIF2α, the major subunit of the translation initiation factor in eukaryotic cells (Donnelly et al., 2013). Phosphorylation of eIF2α inhibits translation, except for a subset of mRNAs including the transcription factor ATF4 which translation is increased (B'chir et al., 2013). ATF4 then activates the transcription of genes involved in stress response. In Drosophila, one of these genes is the eIF4E-binding protein 4E-BP (Kang et al., 2017). 4E-BP activation promotes cap-independent translation, which boosts Anti-Microbial Peptides (AMPs) production in the fat body (Vasudevan et al., 2017) and can alter the composition of the microbiota (Vandehoef et al., 2020). Therefore, we tested whether ATF4 and 4E-BP acting downstream of GCN2 are also necessary for Lp to support larval development upon dietary AA imbalance. We observed that knocking-down ATF4 or 4E-BP in the enterocytes delays the development of GF larvae on an imbalanced diet. However, such knock-downs do not affect the development of Lp-associated larvae like GCN2 knock-down does. ATF4 and 4E-BP are thus not required for Lp to support larval development upon dietary AA imbalance (Fig. 5G). Taken together, our results demonstrate the specific role of the GCN2 pathway in enterocytes to mediates Lp's support to larval development despite dietary AA imbalance, independently of TOR and ATF4.

We then tested the interaction between GCN2 knock-down and Lp r/tRNA loci insertion mutants. As expected, control larvae reared on imbalanced diet in association with r/tRNA mutant F07.08 show a developmental delay compared to larvae associated with WT-like B02.04 (Fig. 5H). On the contrary, larvae knocked-down for GCN2 in the enterocytes do not show a difference between association with F07.08 and association with B02.04 (Fig. 5I); in other words, the effect of the r/tRNA operon mutation is only observed when GCN2 is fully expressed. This suggests a functional interaction between products of the r/t RNAs loci in Lp and GCN2 in the larval gut and supports

the notion that Lp's influence on host adaptation to AA imbalance relies on a molecular
615 dialog engaging symbiont r/tRNAs loci products and the host GCN2 kinase.

Figure 5

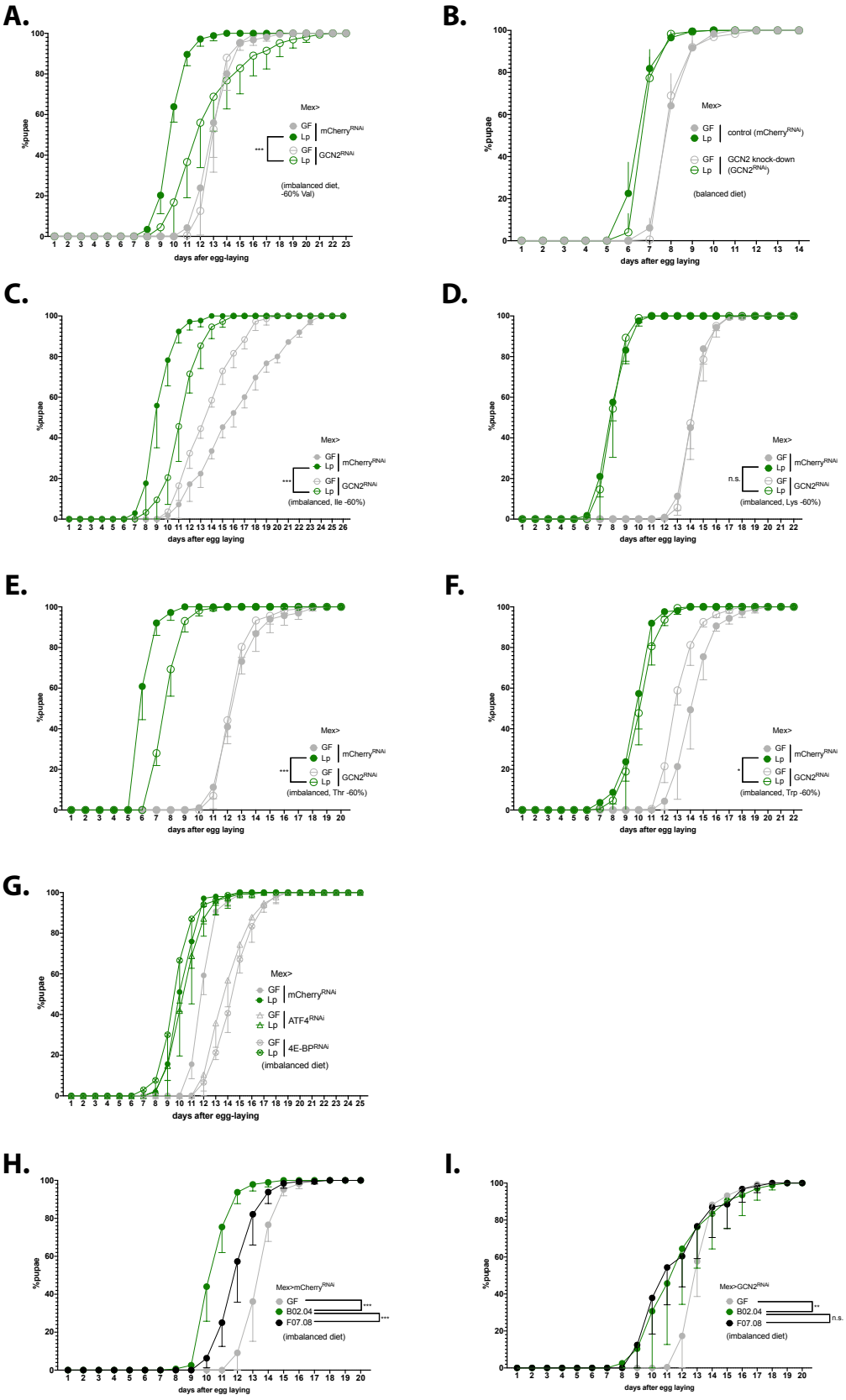

Fig. 5 Expression of GCN2 in the gut is necessary for Lp to rescue the delay due to AA imbalance. **(A-G)** Developmental timing of larvae raised in GF condition (grey circles) or Lp-associated conditions (green circles), in a control background (Mex>mCherry^{RNAi}, filled circles) or in a knock-down background in enterocytes (empty circles). The graphs represent the total fraction of emerged pupae over time as a percentage of the final number of pupae. When indicated, we used a Cox proportional hazards model to compare the effect of Lp in the control background and in the GCN2 knock-down background. n.s.: non-significant. **: p-value<0.01. ***: p-value<0.001. **(A-F)** GCN2 knock-down in the enterocytes on imbalanced diet (-60% Val) **(A)**, balanced diet **(B)** or imbalanced diet: -60% Ile **(C)**, -60% Lys **(D)**, -60% Thr **(E)**, -60% Trp **(F)**. **(G)** ATF4 knock-down in the enterocytes (triangles) and 4E-BP knock-down in enterocytes (crossed circles) on imbalanced diet (-60% Val). **(H-I)** Developmental timing of GF larvae (grey), larvae associated with r/tRNA mutant F07.08 (black) and larvae associated with WT-like mutant B02.04 (green) on imbalanced diet (-60% Val) in a control background (Mex>mCherry^{RNAi}) **(H)** or in a GCN2 knock-down in the enterocytes (Mex>GCN2^{RNAi}) **(I)**. We used a Cox proportional hazards model to compare the effect of B02.04-association with F07.08-association and GF condition. n.s.: non-significant, **: p-value<0.01, ***: p-value<0.001.

Figure S5

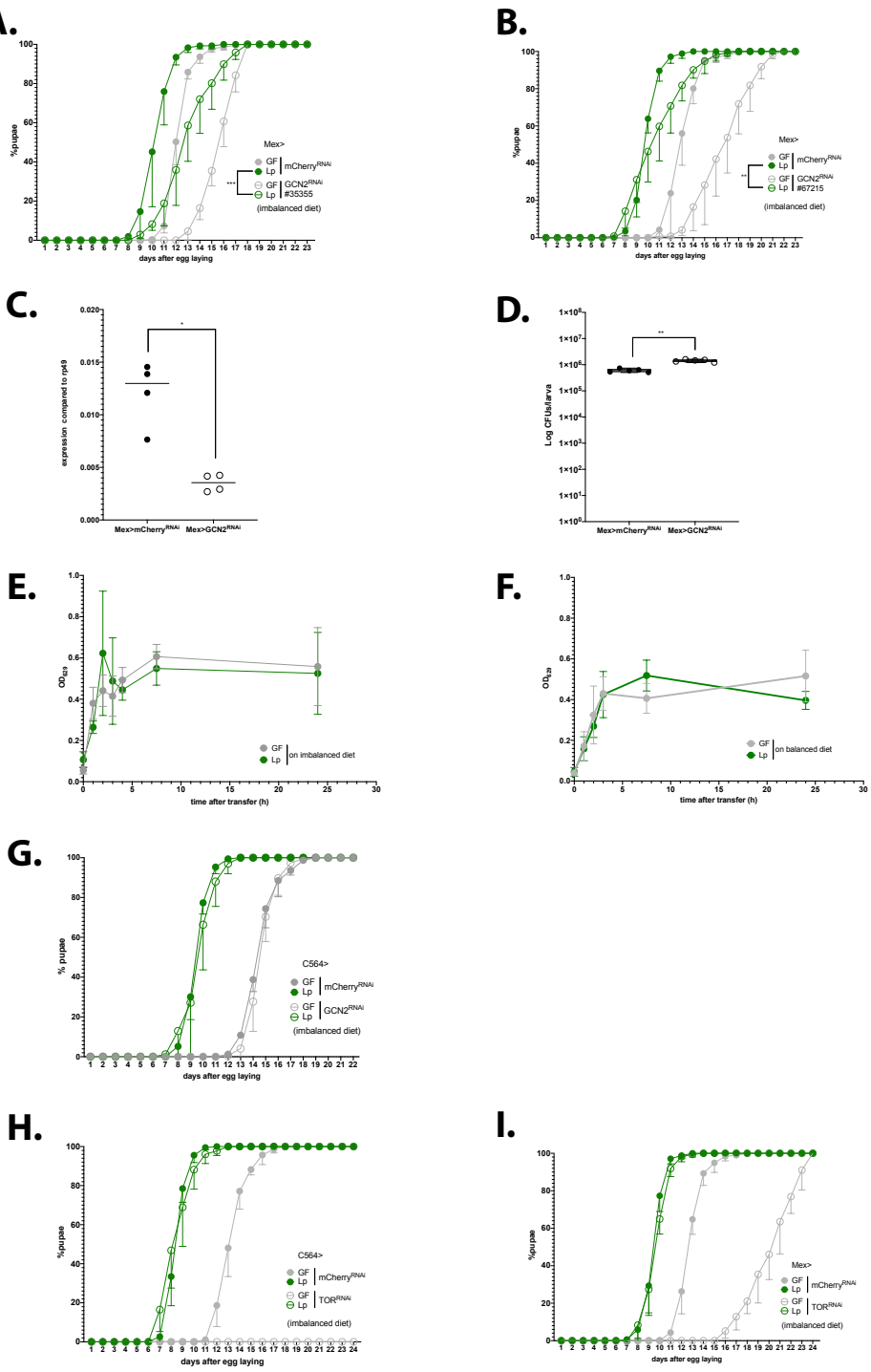

Fig. S5

(A-B) Developmental timing of GF larvae (grey) or Lp-associated larvae (green) from a control background (Mex>mCherry^{RNAi}, filled circles) or GCN2 knock-down larvae (Mex>GCN2^{RNAi}, empty circles). The graph represents the total fraction of emerged pupae over time as a percentage of the final number of pupae. Larvae were reared on imbalanced diet FLY AA -60% Val. We used the lines #BL 35355 **(A)** and #BL 67215 **(B)**. **(C)** Expression of *GCN2* in the anterior midgut of control larvae (Mex>mCherry^{RNAi}) or GCN2 knock-down larvae (Mex>GCN2^{RNAi}). Expression is normalized with the expression of *rp49* using the formula $2^{Cq(rp49)-Cq(GCN2)}$. We performed a Mann-Whitney test to compare

the two conditions, * p-value<0.05. **(D)** Colonization of the gut by Lp in control larvae (Mex>mCherry^{RNAi}, filled circles) or GCN2 knock-down larvae (Mex>GCN2^{RNAi}, empty circles) fed an imbalanced diet (FLY AA -60% Val). The graph shows the quantity of Colony-Forming Units (CFUs) of Lp per larva. We performed a Mann-Whitney test to compare the two conditions. **: p-value<0.01. **(E-F)** Food intake of GF larvae (grey) or Lp-associated larvae (green) reared on balanced diet **(E)** or imbalanced diet **(F)**. Larvae were transferred on coloured food, and food intake was calculated as the Optical Density (OD) of the food ingested by the larvae over time. **(G)** Developmental timing of GF larvae (grey) or Lp-associated larvae (green) from a control background (C564>mCherry^{RNAi}, filled circles) or GCN2 knock-down in the fat body (C564>GCN2^{RNAi}, empty circles). The graph represents the total fraction of emerged pupae over time as a percentage of the final number of pupae. Larvae were reared on imbalanced diet (FLY AA -60% Val). **(H, I)** Developmental timing of GF larvae (grey) or Lp-associated larvae (green) from a control background (mCherry^{RNAi}, filled circles) or TOR knock-down (TOR^{RNAi}, empty circles) in the fat body **(H)** or in the enterocytes **(I)**. The graph represents the total fraction of emerged pupae over time as a percentage of the final number of pupae. Larvae were reared on imbalanced diet (FLY AA -60% Val). GF C564>TOR^{RNAi} larvae did not reach pupariation.

Fig. S6

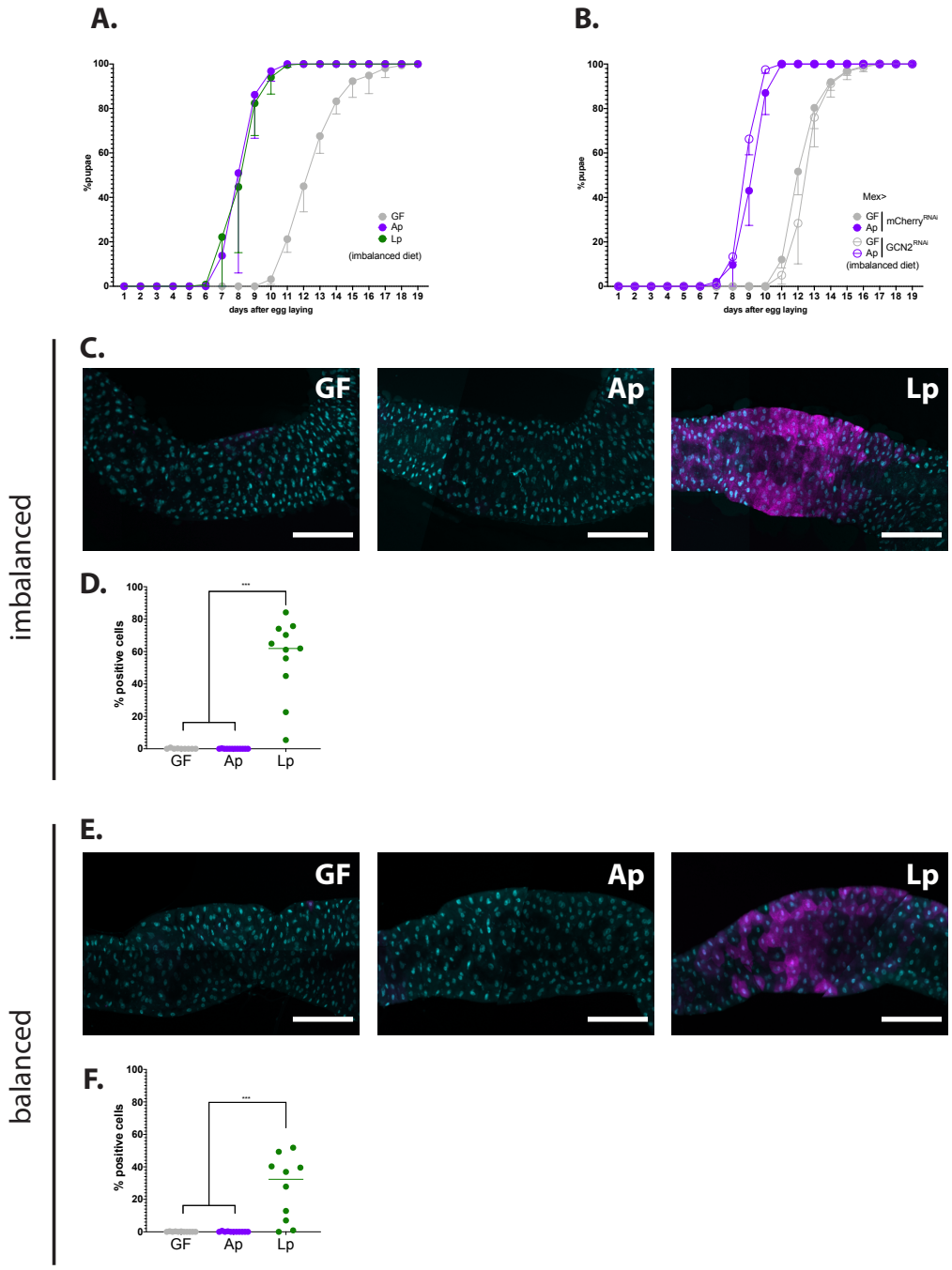

Fig. S6

(A) Developmental timing of larvae raised in GF condition (grey circles), Ap-associated conditions (purple circles) or Lp-associated conditions (green circles) on an imbalanced diet (FLY AA -60% Val). The graph represents the total fraction of emerged pupae over time as a percentage of the final number of pupae. **(B)** Developmental timing of larvae raised in GF condition (grey circles) or Ap-associated conditions (purple circles), in a control background (Mex>mCherry^{RNAi}, filled circles) or in a GCN2 knock-down background (Mex>GCN2^{RNAi}, empty circles) on an imbalanced diet (FLY AA -60% Val). The graph represents the total fraction of emerged pupae over time as a percentage of the final number of pupae. We used a Cox proportional hazards model to compare the effect of Ap in the control background and in the GCN2 knock-down background. n.s.: non-significant. **(C,E)** Representative pictures of the anterior midgut of 4E-BP^{intron}dsRed larvae. Cyan: DAPI. Magenta: 4E-BP^{intron}dsRed reporter. Scale bar: 200 µm.

Left panel: GF larva. Middle panel: Ap-associated larva. Right panel: Lp-associated larva. Larvae were reared on imbalanced diet **(C)** or balanced diet **(E)**. **(D,F)** Quantification of the signal: proportion of enterocytes positive for 4E-BP^{intron}dsRed reporter's activity in the anterior midgut. Each dot represents an independent replicate. The bar shows the mean. We performed a Kruskal-Wallis test followed by post-hoc Dunn's tests to compare GF and Ap to Lp. ***: p-value<0.001. Larvae were reared on imbalanced diet (FLY AA -60% Val) **(D)** or balanced diet (FLY AA) **(F)**.

Discussion

Symbiotic microbes can promote the juvenile growth of their host in nutrient-poor conditions by "enhancing" their nutrition: pea aphids' symbiotic bacteria supplement their host with EAA precursors (Akman Gündüz and Douglas, 2009; Russell et al., 2013); Drosophila's symbiotic bacteria provide B-vitamins and certain EAAs to developing larvae (Consuegra et al., 2020a; Sannino et al., 2018); the microbiota of termites (Brune and Dietrich, 2015), ruminants (Cammack et al., 2018) and rodents (Sakaguchi, 2003) degrades plant fibres otherwise indigestible by their host. Symbiotic microbes can also modify their host's nutrition indirectly: for instance, Lp stimulates the production of digestive enzymes including proteases by Drosophila's enterocytes, which allows the larva to retrieve additional AA from dietary polypeptides (Erkosar et al., 2015; Matos et al., 2017). Here, we reveal an additional symbiotic mechanism supporting host nutrition and growth. We show that the Drosophila bacterial symbiont Lp can rescue the developmental delay of its host due to AA imbalance without 1) providing the limiting AA (because Lp is not capable of synthesizing Val (Consuegra et al., 2020a; Kim et al., 2021; Teusink et al., 2005)) or 2) increasing degradation of dietary polypeptides (because the HD contains only free AA). To understand how Lp promotes adaptation of its host to an imbalanced diet, we performed an unbiased genetic screen and showed that Lp requires operons encoding ribosomal and transfer RNAs to support host growth. We further showed that Lp activates the general control nonderepressible 2 (GCN2) signalling pathway in enterocytes of the anterior midgut, which fosters adaptation to an imbalanced diet and promotes larval growth. GCN2 activation depends on the presence of intact r/tRNAs-encoding operons, and is necessary for Lp to rescue the delay due to AA imbalance. Of note, GCN2 activation in the midgut is not necessary to support growth on a balanced diet, nor when symbiotic bacteria can synthesize the limiting AA (*e.g.* Lp in the context of Lysine scarcity, or Ap upon Valine scarcity). These results therefore reveal a mechanism by which a symbiont supports its host physiological adaptation to a suboptimal nutrition by engaging the host kinase GCN2 in enterocytes, a previously underappreciated function of this signalling module in the gut.

How is GCN2 signalling engaged by Lp?

We showed that GCN2 activation by Lp depends on the presence of the r/tRNA operons. GCN2 is known to be activated by many types of double-stranded RNAs: eukaryotic tRNAs cognate to several AA (Dong et al., 2000), free ribosomal eukaryotic RNA (Zhu and Wek, 1998) and viral RNA (Berlanga et al., 2006). Our results show that

GCN2 can be activated by purified bacterial tRNAs, which make Lp's tRNAs interesting candidates. Of note, one of the mutants (D12.16) shows disruption of an operon that encodes only rRNAs. However, synthesis of tRNAs may be regulated by ribosomal activity (Gourse et al., 1985); therefore, tRNAs production may be indirectly altered in D12.16 as well. Further work is needed to measure how the mutations that we identified impact the synthesis of each family of r/tRNA and to determine which of rRNA, tRNA, other RNA products of the loci or an indirect effect of the r/tRNA operon (for instance, through the translation rate in Lp that may be affected by r/tRNA mutations) is responsible for r/tRNA operon-dependent activation of GCN2 by Lp. Of note, the other two candidates that we identified through the genetic screen might also be linked to r/tRNA production: C08.20 has a transposon insertion of the gene *gnd2* that encodes a phosphogluconate dehydrogenase of the Pentose Phosphate Pathway (PPP). One product of the PPP is the 5-phosphoribosyl-α-1-pyrophosphate (PRPP), which is a precursor for the biosynthesis of nucleotides (Kilstrup et al., 2005). It is thus possible that disruption of *gnd2* in C08.20 might alter production of r/tRNAs by the cells. B12.11 displays an insertion in the end of an operon encoding *rsmC*, *lp_0696* and *lp_sRNA01*. *rsmC* encodes a 16S rRNA methyltransferase. Methylation of rRNA stabilizes ribosomes and improves translation in other bacteria (Wong et al., 2013). *lp_0696* encodes a cytidine/deoxycytidylate deaminase, which catalyses conversion of cytidine into uridine. *lp_sRBA01* encodes the signal recognition particle (SRP), a small non-coding RNA which addresses membrane proteins to the membrane during their translation (Kuhn et al., 2017). Disruption of this operon may thus directly alter RNA production and/or ribosomal function, which can negatively regulate r/tRNA synthesis (Gourse et al., 1985). Several studies have shown that small RNAs from bacteria can act as cues sensed by host cells. tRNAs loci-derived small RNAs from bacteria can regulate host's gene expression in the symbiotic nodules of plants (Ren et al., 2019). The small RNA SsrA is secreted by the symbiont *Vibrio fischeri* and fosters immune tolerance of its host, the squid *Euprymna scolopes* (Moriano-Gutierrez et al., 2020). *Pseudomonas aeruginosa* secretes tRNA-derived small RNAs that inhibit the immune response in cultured human cells and in the mouse lung (Koeppen et al., 2016). Lp is present to the ectoperitrophic space of the gut: it is not in direct contact with the enterocytes (Storelli et al., 2018). Therefore, we do not know how Lp's r/tRNAs may be delivered to enterocytes. *P. aeruginosa*'s sRNAs and *V. fischeri*'s SsrA were found inside extracellular vesicles (Koeppen et al., 2016; Moriano-Gutierrez et al., 2020). Interestingly, *Lacticaseibacillus casei* produces extracellular vesicles that contain r/tRNAs (Domínguez Rubio et al., 2017). Moreover, extracellular vesicles from *Limosilactobacillus reuteri* influence gut motility in mice (West et al., 2020) and extracellular vesicles from *L. plantarum*^{WCFS1} increase the expression of immunity genes in worms and cultured colonocytes (Li et al., 2017). Therefore, we propose a model whereby Lp would deliver r/tRNAs to Drosophila's enterocytes via extracellular vesicles. This model would explain why providing purified tRNAs directly to the larva does not fully recapitulate the effect of Lp on GCN2 activation, as if a vehicle (*i.e.* the extracellular vesicles) was needed.

We showed that GCN2 signalling is activated by Lp in enterocytes of the anterior midgut. This region of the midgut is of particular interest because it is located anteriorly to the acidic zone that kills the majority of Lp cells upon transit. It is thus the main region where enterocytes can interact with live Lp cells (Storelli et al., 2018). The pattern of expression of the 4E-BP^{intron}dsRed reporter slightly differs from the pattern observed by Kang and colleagues (Kang et al., 2017): upon AA scarcity, they observed activation of the reporter in the gastric caeca, the acidic region and the proventriculus like we did, but not in the anterior midgut. Those experiments were done in conventionally-reared larvae where the microbial status of the animals was not reported. We showed that GCN2 activation in the anterior midgut is symbiont-dependent; this difference with our findings thus suggests that the larvae in Kang and colleagues' experiments were associated with bacteria that do not promote GCN2 activation in the anterior midgut, such as Ap. An alternative explanation is that frequently flipped conventional fly stocks or crosses may carry very low microbial titers and therefore present GF-like phenotypes. Of note, we could still observe expression of the 4E-BP^{intron}dsRed reporter in the gastric caeca, the acidic region and the proventriculus upon GCN2 knock-down (whereas GCN2 knock-down completely abolishes 4E-BP^{intron}dsRed expression in the anterior midgut, Fig. 3C-F). This suggests that other ATF4 activators such as PERK are active in the gastric caeca, the acidic region and the proventriculus. Importantly, we observed activation of GCN2 by Lp in both contexts of imbalanced and balanced diet (Fig. 3A,B). We thus identified a GCN2 signalling activation mechanism which is AA-independent but bacteria-dependent. This differs from the canonical GCN2 activation relying on sensing unloaded eukaryotic tRNA upon AA scarcity. Previous studies have observed GCN2 activation in the Drosophila larval gut upon starvation (Kang et al., 2017), upon lack of EAA in adults (Kim et al., 2021) and upon exposure to a high sugar/low protein diet in adults (Bonfini et al., 2021). These observations were made without control over the fly's microbiota, and it is thus difficult to conclude whether bacteria may be at play in these contexts (especially because microbial composition depends largely on diet composition (Lesperance and Broderick, 2020)). Studies have reported activation of GCN2 by pathogenic microbes: infection stimulates GCN2 in the gut, triggers a translational block (Chakrabarti et al., 2012) and promotes immune response through the ATF4-4E-BP axis (Vasudevan et al., 2017). The mechanism of activation of GCN2 by infection was not identified in these studies. Of note, *Shigella* infection causes GCN2 activation in HeLa cells, and it was proposed that GCN2 is activated by AA depletion caused by the intracellular infection (Tattoli et al., 2012). However, this mechanism seems unlikely in our situation because Lp is not intracellular, and because association with Lp actually promotes physiological rescue of AA scarcity. In the light of our results, we suggest that GCN2 may also be activated by r/tRNA or small RNAs produced by pathogenic bacteria upon infection. These studies and ours emphasize the role of GCN2 in the sensing of either pathogenic or symbiotic bacteria, in addition to its role in sensing uncharged eukaryotic tRNAs (Donnelly et al., 2013) and raise the question of the evolutionary history of GCN2 function: could GCN2 have primarily

evolved as a pattern recognition receptor, *i.e.* a sensor for bacterial RNA later co-opted to sense AA scarcity indirectly through sensing uncharged eukaryotic tRNAs?

How does GCN2 activation in the gut support physiological adaptation resulting in improved systemic growth despite imbalanced nutrition?

Our work shows that GCN2 expression in enterocytes is necessary for Lp's support to larval growth on an AA-imbalanced diet. However, overexpression of a constitutively active form of GCN2 in dopaminergic neurons represses growth on an AA-imbalanced diet by inhibiting food intake (Bjordal et al., 2014). These apparently contradictory results suggest that GCN2's action is organ-specific: in neurons, GCN2 may foster adaptation to an imbalanced diet by prompting the larva to find a better food source; whereas in the gut, GCN2 may allow adaptation to an imbalanced diet through physiological changes of enterocytes. In yeasts, GCN2 is induced by AA imbalance and stimulates autophagy and AA transport (Natarajan et al., 2001). Similarly, in cultured mouse fibroblasts, Leucine deprivation results in up-regulation of some AA transporters in a GCN2-dependent manner (Deval et al., 2009). In Drosophila, proteomics analyses comparing WT or GCN2-knocked-down adults found that GCN2 promotes the synthesis of mitochondrial proteins such as components of the electron transport respiratory chain (Kang et al., 2017; Kim et al., 2020). It is therefore also possible that GCN2 activation increases metabolic activity and respiration rates in enterocytes, which would support the high energy-cost of increased nutrient uptake (Boudko, 2012). GCN2 activation by Lp may thus cause an increase in Valine uptake through up-regulation of Valine transporters and/or an increase in Valine recycling through autophagy. Increased Valine uptake and/or recycling would support host systemic growth despite dietary Valine limitation.

Studies in yeast's or Drosophila's GCN2 pathway have focused on the effector ATF4, which translation increases upon eIF2α's phosphorylation by GCN2. Especially, Vasudevan and colleagues showed than the GCN2-ATF4-4E-BP cascade yields the production of Anti-Microbial Peptides that help Drosophila fight infection (Vasudevan et al., 2017). Here, although we did indirectly observe activation of ATF4 (Fig. 3) and 4E-BP (Fig. S3C) upon Lp-association, this activation is not necessary for Lp to rescue the effects of AA imbalance. Adaptation to AA imbalance may occur independently of eIF2α, through other substrates of GCN2. eIF2α is the only known substrate of GCN2; however, Dang Do and colleagues showed that in the mouse liver, GCN2 does not regulate the same set of genes as PERK, another eIF2α-kinase. This suggests that additionally to their common substrate eIF2α, GCN2 and PERK have distinct substrates (Dang Do et al., 2009). eIF2α-independent action of GCN2 was described in response to UV exposure (Grallert and Boye, 2007) and viral infection (Krishnamoorthy et al., 2008). Alternatively, support to growth despite AA imbalance by Lp may rely on eIF2α targets other than ATF4. ATF4-independent regulation of gene expression by eIF2α was described in Drosophila (Malzer et al., 2018), mice

(Guo and Cavener, 2007) and cultured Mammalian cells (Harding et al., 2003; Wek and Cavener, 2007). Interestingly, GCN2, but not ATF4, is necessary for adaptation of mice to a Leucine-depleted diet (Zhang et al., 2002). Further work is needed to unravel GCN2-dependent/ATF4-independent adaptation to AA imbalance.

In conclusion, we showed that the symbiotic bacterium Lp can rescue the effects of AA imbalance on growth through GCN2 activation in enterocytes, possibly through direct sensing of products of r/tRNAs operons. GCN2 is highly conserved across Eukaryotes (Donnelly et al., 2013), and is important for mouse adaptation to an AA-imbalanced diet (Anthony et al., 2004; Guo and Cavener, 2007; Laeger et al., 2016; Zhang et al., 2002). Our study therefore paves the way to testing whether the molecular dialogue between symbiotic bacteria and GCN2 described here is also at play in juvenile mammals suffering from malnutrition.

Material and Methods

Drosophila lines and breeding

Drosophila stocks were maintained at 25°C with 12:12-h dark/light cycles on a yeast/cornmeal medium composed of 50 $g.L^{-1}$ of inactivated yeast, 80 $g.L^{-1}$ of cornmeal, 4 $mL.L^{-1}$ of propionic acid, 5.2 $g.L^{-1}$ of nipagin and 7.14 $g.L^{-1}$ of agar. All experiments were conducted in gnotobiotic flies derived from GF stocks. GF stocks were established as previously described (Combe et al., 2014) and maintained on yeast/cornmeal medium supplemented with antibiotics (50 µg/mL of kanamycin, 50 µg/mL of ampicilin, 10 µg/mL of tetracyclin and 5 µg/mL of erythromycin). We verified axenicity by grinding GF flies using a Precellys 24 tissue homogenizer (Bertin Technologies, Montigny-le-Bretonneux, France) and plating the lysate on Man-Rogosa-Sharp (MRS) Agar (Carl Roth, Karlsruhe, Germany) and LB Agar (Carl Roth, Karlsruhe, Germany). We used *yw* flies (BDSC #1495) as a reference strain. The following lines were used: UAS-mCherry^{RNAi} (BDSC #35785), UAS-TOR^{RNAi} (BDSC #33951), UAS-GCN2^{RNAi}-1 (VRDC #103976 obtained from P. Leopold's lab. This line was used for all GCN2 knock-downs unless specified otherwise), UAS-GCN2^{RNAi}-2 (BDSC #35355), UAS-GCN2^{RNAi}-3 (BDSC 67215), UAS-ATF4^{RNAi} (VDRC #109014), UAS-4E-BP^{RNAi} (VDRC #36667), 4E-BP^{intron}dsRed (obtained from H.D. Ryoo's lab), Mex1-Gal4 and C564-Gal4 from out stocks. We generated the line 4E-BP^{intron}dsRed, UAS-GCN2^{RNAi} by recombining the lines 4E-BP^{intron}dsRed and UAS-GCN2^{RNAi}-1.

Holidic diets

The holidic diets (HDs) were prepared following the protocol of Piper and colleagues (Piper, 2017) at a total AA concentration of 10.7 $g.L^{-1}$. We made two changes to Piper and colleagues' protocol: we used a lower concentration of sucrose (5 $g.L^{-1}$) because we noted that this concentration is the best for GF larvae: higher sucrose concentrations are toxic and slightly delay development of GF larvae (data not shown).

Moreover, we omitted the conservatives (propionic acid or nipagin) because they can alter bacterial growth. We worked in sterile conditions: tubes and egg-laying cages were UV-treated or autoclaved, and solutions were either autoclaved (first part containing agar, Leu, Ile, Tyr, sucrose, cholesterol and traces, as well as the acetate buffer solution) or filter-sterilized (stock solutions of EAA, NEAA, Glu, Cys, Vitamins, Nucleic Acids and Lipids precursors, Folate). For all experiments involving transposon mutants, we supplemented the HD with Erythromycin (5 µg.mL^{-1}). HD was stored at 4°C for maximum one week before use.

Bacteria and culture conditions

We used the strain Lp^{NC8} of *Lactiplantibacillus plantarum* and the strain Ap^{WJL} of *Acetobacter pomorum*. Conversely to other strains of *L. plantarum*, Lp^{NC8} was not isolated from a fly but from grass silage (Axelsson et al., 2012); we used it because it is as growth promoting as fly isolates and it can be efficiently targeted for genetic modifications (Matos et al., 2017). Lp^{NC8} was grown overnight at 37°C without agitation in MRS Broth Medium (Carl Roth, Karlsruhe, Germany). The Lp mutant library was generated by random transposon insertion from Lp^{NC8} (Matos et al., 2017). All Lp transposon insertion mutants were grown for 24h in MRS supplemented with Erythromycin at 5 µg.mL^{-1}. The Lp^{GFP} strain was generated from Lp^{WJL} (Ryu et al., 2008; Storelli et al., 2018). Lp^{GFP} was grown for 24h in MRS supplemented with Chloramphenicol at 10 µg.mL^{-1}. Ap^{WJL} was isolated from a fly's intestine (Ryu et al., 2008). Ap^{WJL} was grown for 24h in Mannitol Broth composed of 3 g.L^{-1} of Bacto peptone (Becton Dickinson), 5 g.L^{-1} of yeast extract (Becton Dickinson) and 25 g.L^{-1} of D-mannitol (Carl Roth) in a flask at 30˚C under 180 rpm agitation.

Developmental timing experiments

GF flies were placed in a sterile breeding cage overnight to lay eggs on a dish of HD similar to the HD used for the experiment. At d0, we collected the eggs and placed them in the tubes containing the HD. Unless stated otherwise, each experimental condition consisted in 5 tubes each containing 40 eggs. Eggs were then inoculated with 100 µL of sterile PBS 1X (GF condition) or with 100 µL of a culture of bacteria resuspended in PBS 1X (yielding ~2x10^8 CFUs of Lp and ~10^7 CFUs of Ap per tube). For the Heat-Killed (HK) condition, the resuspension of Lp in PBS was incubated 3h at 65°C. After inoculation, the larvae were kept at 25°C with 12:12-h dark/light cycles. The number of newly emerged pupae was scored every day until all pupae have emerged. The data are represented either as curves of pupariation over time or as the median time of pupariation (D50) calculated using the D50App (http://paulinejoncour.shinyapps.io/D50App). We used the R package *Coxme* (Therneau and Grambsch, 2000) to make a Cox proportional hazard model adapted to curves of pupariation over time, replacing the event "death" with the event "pupariation" (Rodrigues et al., 2021). Each experiment was performed in five independent replicates (one replicate consists in a tube containing 40 eggs as

explained above). To compare the effect of Lp on development across different diets (*e.g.* balanced HD vs imbalanced HD), we tested whether the interaction between absence/presence of Lp and the diet was significant using the model *pupariation ~absence/presence of Lp * diet + (1|Replicate)* (1|Replicate accounts for replicates as a random factor). When necessary, we used the FDR method to correct for multiple comparisons. To compare one treatment to other treatments (*e.g.* to compare the developmental timing of B02.04-associated larvae with GF larvae and F07.08-associated larvae), we performed a general linear hypotheses test (glht) from the package *multcomp* (Hothorn et al., 2008) using Tukey post hoc pairwise comparisons.

Genetic screen

The genetic screen was performed in the same conditions as other Developmental timing experiments, but we used 20 eggs per condition in small tubes and one replicate per condition. Each condition consisted in the inoculation of one transposon insertion mutant. The screen was divided into four batches. For each batch, we calculated the D50 of each mutant, and the associated z-score. We then pooled the z-scores from the four batches and selected the ones above a threshold of 2.5. The 32 candidates were re-tested in a Developmental timing experiment of 5 replicates. We compared the candidates to the WT-like transposon insertion mutant B02.04 from the library (transposon inserted in an intergenic region downstream *dnaJ*).

Mapping of insertions by Whole Genome Sequencing (WGS)

The transposons inserted in the mutant's genomes are not bar-coded. To map them, we extracted the genomic DNA of each candidate using a kit UltraClean Microbial DNA isolation (MoBio, Jefferson City, Missouri, USA). Samples were quality-checked using a Qubit 4.0 HS DNA. To sequence genomic bacterial DNA, libraries were built using the Nextera DNA Flex Library Prep (Illumina, San Diego, California, USA) starting from 500 ng of DNA (except for 2 samples for which 350 ng and 280 ng were used) and following the provider's recommendations. The 17 dual-indexed libraries were pooled in an equimolar manner and sequenced on a paired-end mode (2x75bp) using a NextSeq500 Illumina sequencer and a mid-output run. More than 155M of reads were obtained for the run generating between 7M to 12M of reads by sample. Data were analyzed using Galaxy (Afgan et al., 2016). Briefly, for each mutant, we filtered all pairs of reads which had one of the two reads mapped on the transposon sequence. We gathered the paired reads and mapped them on the genome of Lp^{NC8} (Axelsson et al., 2012) to identify the region in contact of the transposon. The genome of Lp^{NC8} contains five operons encoding r/tRNAs that share high sequence similarities. Therefore, sequencing did not allow us to identify in which operon the insertion took place. We thus used operon-specific PCR to identify in which operon the transposon was inserted for each mutant. For each mutant, we used two primers specific of the transposon (OLB215 and OLB 221) and one primer specific of each r/t RNA operon (op1, op2,

op3, op4 and op5). The sequences of all primers used in this study can be found in Table S1.

Construction of LpΔop$_{r/tRNA}$

We deleted the operon encoding rRNA 5S, 16S and 23S as well as tRNAs for Ala, Ile, Asn and Thr that was independently identified in two insertion mutants from the genetic screen (C09.09 and F07.08, see Fig. 2G). We used homology-based recombination with double-crossing over as described in (Matos et al., 2017). Briefly, Lp^{NC8}'s chromosomic DNA was purified with a kit UltraClean Microbial DNA isolation (MoBio, Jefferson City, Missouri, USA). The regions upstream and downstream of the operon were then amplified using Q5 High-Fidelity 2X Master Mix (New England Biolabs, Ipswich, Massachusetts, USA) with the following primers that contain overlapping regions with the plasmid pG+host9 (Maguin et al., 1996) to allow for Gibson Assembly: tRNAop_1, tRNAop_2, tRNAop_3 and tRNAop_4 (Table S1). The PCR fragments were inserted into the plasmid pG+host9 digested with PstI (New England Biolabs, Ipswich, Massachusetts, USA) by Gibson Assembly (New England Biolabs, Ipswich, Massachusetts, USA) and transformed into *E. coli* VE14188. The plasmid was purified and transformed into *E. coli* VE14188 $\Delta dam\Delta dcm$ to demethylate the DNA. The plasmid was then purified and transformed into Lp^{NC8} by electroporation. Transformants were grown in MRS supplemented with Erythromycin at 5 µg.mL^{-1} at 42°C, which does not allow replication of the plasmid, in order to select integration of the plasmid into the chromosome by crossing-over. Plasmid excision associated with deletion of the operon by a second crossing-over event was then obtained by sub-culturing Lp in absence of Erythromycin. The deletion was screened by colony PCR and confirmed by sequencing using the primers tRNAop_5 and tRNAop_6 (Table S1).

Microscopy

4E-BP^{intron}dsRed larvae were reared on HD as described for Developmental timing experiments. We collected them at pre-wandering mid-L3, 1 day before the emergence of the first pupae (typically D5 after egg-laying (AEL) for Lp-associated larvae on balanced diet, D6 AEL for Lp-associated larvae on imbalanced diet or GF larvae on balanced diet, D7 AEL for GCN2 knocked-down Lp-associated larvae on imbalanced diet, D10 AEL for GF larvae on imbalanced diet, D6 AEL for B02.04-associated larvae on imbalanced diet and D8 AEL for F07.08-associated larvae on imbalanced diet). For short-term association, GF larvae were reared on imbalanced diet until D8 AEL, associated with B02.04 and F07.08 as previously described and collected at D10 AEL. Larvae were dissected in PBS 1X. The guts were fixed in paraformaldehyde (PFA) 4% in PBS 1X 1h at room temperature, washed in PBS 1X, washed three times in PBS Triton 0.2%, washed in PBS1X and mounted in ROTI®Mount FluorCare DAPI (Carl Roth, Karlsruhe, Germany). Pictures were acquired with a confocal microscope Zeiss LSM 780 (Zeiss, Oberkochen, Germany). We analysed the images on Fiji (Schindelin et al., 2012) using a custom macro: the macro identifies the reporter-positive regions

above a defined threshold in the anterior midgut, and count the number of DAPI-positive particles inside these regions. It then counts the total number of DAPI-positive particles in the anterior midgut and uses it for normalization.

Bacterial growth on HD

Microtubes containing 400 µL of imbalanced HD were inoculated with ~10^6 CFUs of each candidate mutant. 5 L1 GF larvae were added to each tube, and the tubes were incubated at 25°C. Each day, 3 samples per condition were collected for CFUs counting: we added 600 µL of sterile PBS 1X and grinded them using a Precellys 24 tissue homogenizer (Bertin Technologies, Montigny-le-Bretonneux, France. Settings: 6000 rpm, 2x30s, 30s pause). The homogenates were diluted at the appropriate concentration and plated on MRS Agar using an Easyspiral automatic plater (Interscience, Saint-Nom-la-Breteche, France). Plates were incubated at 37°C for 48h, and the number of CFUs was assessed using an automatic colony counter Scan1200 (Interscience, Saint-Nom-la-Breteche, France) and its counting software.

Colonization of the larval gut

Larvae were reared on imbalanced diet as for Developmental timing experiments. 6 days AEL, larvae were collected, surface-sterilized in ethanol 70% and grinded using a Precellys 24 tissue homogenizer (Bertin Technologies, Montigny-le-Bretonneux, France. Settings: 6000 rpm, 2x30s, 30s pause). The CFUs were then counted as described above.

tRNAs feeding

4E-BP^{intron}dsRed larvae were reared on balanced diet as for Developmental timing experiments. At d0, d2, d4 and d5 AEL, the tubes were supplemented with 50 µL of a solution of tRNAs dissolved in Millipore water to reach a total concentration in the tube of 5, 25 and 125 µg.mL^{-1}. GF controls were supplemented with the same volume of Millipore water. We purchased the purified tRNAs at Sigma-Aldricht (Saint-Louis, Missouri, USA; bacterial tRNAs from *Escherichia coli* 10109541001, eukaryotic tRNAs from yeast 10109517001). Larvae were dissected 6 days AEL and treated as described above.

Food intake experiments

Larvae were reared on holidic diet as described for Developmental timing experiments. Larvae were collected 1 day before the emergence of the first pupae and placed on holidic diet containing Erioglaucine disodium salt (Sigma-Aldrich, Saint-Louis, Missouri, USA) at 0.8%. Every hour, we collected 5 larvae in 5 replicates per condition, rinsed them in PBS and placed them in a microtube with beads and 500 µL PBS. Larvae were grinded using a Precellys 24 tissue homogenizer (Bertin Technologies,

Montigny-le-Bretonneux, France. Settings: 6000 rpm, 2x30s, 30s pause). Optical Density at 0.629 nm was measured using a spectrophotometer SPECTROstarNano (BMG Labtech GmbH, Ortenberg, Germany).

RNA extraction

Larvae were reared as described for Developmental timing experiments and collected 1 day before the emergence of the first pupae. Larvae were dissected in PBS, and dissected anterior midguts were kept in RNAlater (Thermofisher, Waltham, Massachusetts, USA) before they were transferred to a microtube and flash-frozen. We used 10 guts for each replicate, and made 5 replicates for each condition. Samples were grinded using a Precellys 24 tissue homogenizer (Bertin Technologies, Montigny-le-Bretonneux, France. Settings: 6500 rpm, 2x30s, 30s pause) and total RNA was extracted using a RNeasy kit (Macherey-Nagel, Hoerdt, France) following the instructions of the manufacturer.

RT-qPCR

We adjusted RNA concentrations and performed Reverse-Transcription (RT) on extracted RNAs using a SuperScript II RT kit (Thermofisher, Waltham, Massachusetts, USA) and random primers (Invitrogen, Waltham, Massachusetts, USA) following the instructions of the manufacturer. We then performed quantitative PCR using the primers GCN2-forward, GCN2-reverse, 4E-BP-forward, 4E-BP-reverse, rp49-forward and rp49-reverse (Table S1) using SYBR GreenER qPCR Supermix (Invitrogen, Waltham, Massachusetts, USA).

Figures and statistics

Figures were created using the Prism GraphPad software and Biorender (BioRender.com). Statistical analyses were performed using the Prism GraphPad software and RStudio.

Table S1	
name	**sequence**
OLB215	ATGGCCGCGGGATTACGACTCC
OLB221	AGCTATGCATCCAACGCGTTGGG
op1	CAAACGGGTGCTGGATGAAA
op2	TTAGCCCAGGACTTGCAAGA
op3	AGGAAGTTACCCCGAACCTG
op4	GCTAGATTTCCGGCACACTG
op5	GAAGGCGGATGGGACTAAGT
tRNAop_1	TGGATCCCCCGGGCTGCACTGACGATGGCATTGTCACT

tRNAop_2	CCTCACAAGGATGAGTTCTAAAAAGCTCA
tRNAop_3	GAACTCATCCTTGTGAGGTGGGACGTGG
tRNAop_4	TGATATCGAATTCCTGCAAGGCTAGCAGAACTTAAATTCTTCT
tRNAop_5	ATGGACCGGAACATAATCC
tRNAop_6	TGGAGTCAAGATAACAAGCG
GCN2-forward	TGGCGCCCCTAGATGGCTCAATCCCAAGAGCTACG
GCN2-reverse	TAGCCTCCCTAGCGCGGAAGTAGAGCGTCTCCGTG
4E-BP-forward	CAGATGCCCGAGGTGTACTC
4E-BP-reverse	CATGAAAGCCCGCTCGTAGA
rp49-forward	GACGCTTCAAGGGACAGTATCTG
rp49-reverse	AAACGCGGTTCTGCATGA

Table S1
Primers used in this study.

Acknowledgements

We would like to thank Pr. Hyung Don Ryoo, Dr. Pierre Leopold, Dr. Nathalie Arquier, the Vienna Drosophila Resource Center and the Bloomington Stock Center for fly lines; Dr. David Duneau for his help with statistical analyses; Lucie Fallone and Meline Garcia for their help with experiments; the ArthroTools platform and the PLATIM platform of the SFR Biosciences (UAR3444/US8) for fly facility and microscopy equipments. Research in F. Leulier's lab is supported by the "Fondation pour la Recherche Médicale" (« Equipe FRM DEQ20180339196) and the Scientific Breakthrough Project from Université de Lyon "Microbehave". T. Grenier is funded by a PhD fellowship from ENS de Lyon. J. Consuegra is funded by a postdoctoral fellowship from the ''Fondation pour la Recherche Médicale'' (FRM, SPF20170938612).

References

Afgan, E., Baker, D., van den Beek, M., Blankenberg, D., Bouvier, D., Čech, M., Chilton, J., Clements, D., Coraor, N., Eberhard, C., et al. (2016). The Galaxy platform for accessible, reproducible and collaborative biomedical analyses: 2016 update. Nucleic Acids Res *44*, W3–W10.

Akman Gündüz, E., and Douglas, A.E. (2009). Symbiotic bacteria enable insect to use a nutritionally inadequate diet. Proc Biol Sci *276*, 987–991.

Anthony, T.G., McDaniel, B.J., Byerley, R.L., McGrath, B.C., Cavener, D.R., McNurlan, M.A., and Wek, R.C. (2004). Preservation of liver protein synthesis during dietary leucine deprivation occurs at the expense of skeletal muscle mass in mice deleted for eIF2 kinase GCN2. J Biol Chem *279*, 36553–36561.

Armstrong, A.R., Laws, K.M., and Drummond-Barbosa, D. (2014). Adipocyte amino acid

sensing controls adult germline stem cell number via the amino acid response pathway and independently of Target of Rapamycin signaling in Drosophila. Development *141*, 4479–4488.

Axelsson, L., Rud, I., Naterstad, K., Blom, H., Renckens, B., Boekhorst, J., Kleerebezem, M., van Hijum, S., and Siezen, R.J. (2012). Genome sequence of the naturally plasmid-free *Lactobacillus plantarum* strain NC8 (CCUG 61730). J Bacteriol *194*, 2391–2392.

Battley, E.H. (1988). Escherichia Coli and Salmonella Typhimurium. Cellular and Molecular Biology, Volume 1; Volume 2. Frederick C. Neidhardt , John L. Ingraham , Boris Magasanik , K. Brooks Low , Moselio Schaechter , H. Edwin Umbarger. The Quarterly Review of Biology *63*, 463–464.

B'chir, W., Maurin, A.-C., Carraro, V., Averous, J., Jousse, C., Muranishi, Y., Parry, L., Stepien, G., Fafournoux, P., and Bruhat, A. (2013). The eIF2α/ATF4 pathway is essential for stress-induced autophagy gene expression. Nucleic Acids Res *41*, 7683–7699.

Berlanga, J.J., Ventoso, I., Harding, H.P., Deng, J., Ron, D., Sonenberg, N., Carrasco, L., and de Haro, C. (2006). Antiviral effect of the mammalian translation initiation factor 2alpha kinase GCN2 against RNA viruses. EMBO J *25*, 1730–1740.

Bjordal, M., Arquier, N., Kniazeff, J., Pin, J.P., and Léopold, P. (2014). Sensing of Amino Acids in a Dopaminergic Circuitry Promotes Rejection of an Incomplete Diet in Drosophila. Cell *156*, 510–521.

Blanton, L.V., Charbonneau, M.R., Salih, T., Barratt, M.J., Venkatesh, S., Ilkaveya, O., Subramanian, S., Manary, M.J., Trehan, I., Jorgensen, J.M., et al. (2016). Gut bacteria that prevent growth impairments transmitted by microbiota from malnourished children. Science *351*, aad3311.

Bonfini, A., Dobson, A.J., Duneau, D., Revah, J., Liu, X., Houtz, P., and Buchon, N. (2021). Multiscale analysis reveals that diet-dependent midgut plasticity emerges from alterations in both stem cell niche coupling and enterocyte size. ELife *10*, e64125.

Boudko, D.Y. (2012). Molecular basis of essential amino acid transport from studies of insect nutrient amino acid transporters of the SLC6 family (NAT-SLC6). Journal of Insect Physiology *58*, 433–449.

Brune, A., and Dietrich, C. (2015). The Gut Microbiota of Termites: Digesting the Diversity in the Light of Ecology and Evolution. Annual Review of Microbiology *69*, 145–166.

Cammack, K.M., Austin, K.J., Lamberson, W.R., Conant, G.C., and Cunningham, H.C. (2018). Ruminant nutrition symbosium: Tiny but mighty: the role of the rumen microbes in livestock production. J. Anim. Sci. *96*, 752–770.

Castro-Portuguez, R., and Sutphin, G.L. (2020). Kynurenine pathway, NAD+ synthesis, and mitochondrial function: Targeting tryptophan metabolism to promote longevity and healthspan. Exp Gerontol *132*, 110841.

Chakrabarti, S., Liehl, P., Buchon, N., and Lemaitre, B. (2012). Infection-Induced Host

Translational Blockage Inhibits Immune Responses and Epithelial Renewal in the Drosophila Gut. Cell Host & Microbe *12*, 60–70.

Colombani, J., Raisin, S., Pantalacci, S., Radimerski, T., Montagne, J., and Léopold, P. (2003). A Nutrient Sensor Mechanism Controls Drosophila Growth. Cell *114*, 739–749.

Combe, B.E., Defaye, A., Bozonnet, N., Puthier, D., Royet, J., and Leulier, F. (2014). *Drosophila* microbiota modulates host metabolic gene expression via IMD/NF-κB signaling. PLoS One *9*.

Consuegra, J., Grenier, T., Baa-Puyoulet, P., Rahioui, I., Akherraz, H., Gervais, H., Parisot, N., Silva, P. da, Charles, H., Calevro, F., et al. (2020a). Drosophila-associated bacteria differentially shape the nutritional requirements of their host during juvenile growth. PLOS Biology *18*, e3000681.

Consuegra, J., Grenier, T., Akherraz, H., Rahioui, I., Gervais, H., da Silva, P., and Leulier, F. (2020b). Metabolic Cooperation among Commensal Bacteria Supports Drosophila Juvenile Growth under Nutritional Stress. IScience *23*, 101232.

Dang Do, A.N., Kimball, S.R., Cavener, D.R., and Jefferson, L.S. (2009). eIF2α kinases GCN2 and PERK modulate transcription and translation of distinct sets of mRNAs in mouse liver. Physiol Genomics *38*, 328–341.

Deval, C., Chaveroux, C., Maurin, A.-C., Cherasse, Y., Parry, L., Carraro, V., Milenkovic, D., Ferrara, M., Bruhat, A., Jousse, C., et al. (2009). Amino acid limitation regulates the expression of genes involved in several specific biological processes through GCN2-dependent and GCN2-independent pathways. FEBS J *276*, 707–718.

Dever, T.E., Feng, L., Wek, R.C., Cigan, A.M., Donahue, T.F., and Hinnebusch, A.G. (1992). Phosphorylation of initiation factor 2α by protein kinase GCN2 mediates gene-specific translational control of GCN4 in yeast. Cell *68*, 585–596.

Dietzl, G., Chen, D., Schnorrer, F., Su, K.-C., Barinova, Y., Fellner, M., Gasser, B., Kinsey, K., Oppel, S., Scheiblauer, S., et al. (2007). A genome-wide transgenic RNAi library for conditional gene inactivation in Drosophila. Nature *448*, 151–156.

Domínguez Rubio, A.P., Martínez, J.H., Martínez Casillas, D.C., Coluccio Leskow, F., Piuri, M., and Pérez, O.E. (2017). Lactobacillus casei BL23 Produces Microvesicles Carrying Proteins That Have Been Associated with Its Probiotic Effect. Front Microbiol *8*.

Dong, J., Qiu, H., Garcia-Barrio, M., Anderson, J., and Hinnebusch, A.G. (2000). Uncharged tRNA Activates GCN2 by Displacing the Protein Kinase Moiety from a Bipartite tRNA-Binding Domain. Molecular Cell *6*, 269–279.

Donnelly, N., Gorman, A.M., Gupta, S., and Samali, A. (2013). The eIF2α kinases: their structures and functions. Cell Mol Life Sci *70*, 3493–3511.

Erkosar, B., Storelli, G., Defaye, A., and Leulier, F. (2013). Host-intestinal microbiota mutualism: "learning on the fly." Cell Host & Microbe *13*, 8–14.

Erkosar, B., Storelli, G., Mitchell, M., Bozonnet, L., Bozonnet, N., and Leulier, F. (2015).

Pathogen virulence impedes mutualist-mediated enhancement of host juvenile growth via inhibition of protein digestion. Cell Host Microbe *18*, 445–455.

Gallinetti, J., Harputlugil, E., and Mitchell, J.R. (2013). Amino acid sensing in dietary-restriction-mediated longevity: roles of signal-transducing kinases GCN2 and TOR. Biochem J *449*, 1–10.

Goberdhan, D.C.I., Wilson, C., and Harris, A.L. (2016). Amino Acid Sensing by mTORC1: Intracellular Transporters Mark the Spot. Cell Metab *23*, 580–589.

Gould, A.L., Zhang, V., Lamberti, L., Jones, E.W., Obadia, B., Korasidis, N., Gavryushkin, A., Carlson, J.M., Beerenwinkel, N., and Ludington, W.B. (2018). Microbiome interactions shape host fitness. Proc. Natl. Acad. Sci. U.S.A. *115*, E11951–E11960.

Gourse, R.L., Takebe, Y., Sharrock, R.A., and Nomura, M. (1985). Feedback regulation of rRNA and tRNA synthesis and accumulation of free ribosomes after conditional expression of rRNA genes. Proc Natl Acad Sci U S A *82*, 1069–1073.

Grallert, B., and Boye, E. (2007). The Gcn2 Kinase as a Cell Cycle Regulator. Cell Cycle *6*, 2768–2772.

Grasmann, G., Smolle, E., Olschewski, H., and Leithner, K. (2019). Gluconeogenesis in cancer cells – repurposing of a starvation-induced metabolic pathway? Biochim Biophys Acta Rev Cancer *1872*, 24–36.

Guo, F., and Cavener, D.R. (2007). The GCN2 eIF2α Kinase Regulates Fatty-Acid Homeostasis in the Liver during Deprivation of an Essential Amino Acid. Cell Metabolism *5*, 103–114.

Harding, H.P., Zhang, Y., Zeng, H., Novoa, I., Lu, P.D., Calfon, M., Sadri, N., Yun, C., Popko, B., Paules, R., et al. (2003). An Integrated Stress Response Regulates Amino Acid Metabolism and Resistance to Oxidative Stress. Molecular Cell *11*, 619–633.

Heitman, J., Movva, N.R., and Hall, M.N. (1991). Targets for cell cycle arrest by the immunosuppressant rapamycin in yeast. Science *253*, 905–909.

Hinton, T., Noyes, D.T., and Ellis, J. (1951). Amino acids and growth factors in a chemically defined medium for *Drosophila*. Physiological Zoology *24*, 335–353.

Hothorn, T., Bretz, F., and Westfall, P. (2008). Simultaneous inference in general parametric models. Biom J *50*, 346–363.

Jugder, B.-E., Kamareddine, L., and Watnick, P.I. (2021). Microbiota-derived acetate activates intestinal innate immunity via the Tip60 histone acetyltransferase complex. Immunity S1074-7613(21)00223-5.

Kamareddine, L., Robins, W.P., Berkey, C.D., Mekalanos, J.J., and Watnick, P.I. (2018). The *Drosophila* Immune Deficiency Pathway Modulates Enteroendocrine Function and Host Metabolism. Cell Metabolism.

Kang, M.-J., Vasudevan, D., Kang, K., Kim, K., Park, J.-E., Zhang, N., Zeng, X., Neubert, T.A., Marr, M.T., and Ryoo, H.D. (2017). 4E-BP is a target of the GCN2–ATF4 pathway during Drosophila development and aging. J Cell Biol *216*, 115–129.

Keebaugh, E.S., Yamada, R., Obadia, B., Ludington, W.B., and Ja, W.W. (2018). Microbial quantity impacts *Drosophila* nutrition, development, and lifespan. IScience *4*, 247–259.

Kilstrup, M., Hammer, K., Ruhdal Jensen, P., and Martinussen, J. (2005). Nucleotide metabolism and its control in lactic acid bacteria. FEMS Microbiology Reviews *29*, 555–590.

Kim, B., Kanai, M.I., Oh, Y., Kyung, M., Kim, E.-K., Jang, I.-H., Lee, J.-H., Kim, S.-G., Suh, G.S.B., and Lee, W.-J. (2021). Response of the microbiome–gut–brain axis in Drosophila to amino acid deficit. Nature 1–5.

Kim, K., Park, J.-E., Yeom, J., Park, N., Trần, T.-X.T., and Kang, M.-J. (2020). Tissue-specific roles of GCN2 in aging and autosomal dominant retinitis pigmentosa. Biochem Biophys Res Commun *533*, 1054–1060.

Koeppen, K., Hampton, T.H., Jarek, M., Scharfe, M., Gerber, S.A., Mielcarz, D.W., Demers, E.G., Dolben, E.L., Hammond, J.H., Hogan, D.A., et al. (2016). A Novel Mechanism of Host-Pathogen Interaction through sRNA in Bacterial Outer Membrane Vesicles. PLOS Pathogens *12*, e1005672.

Krishnamoorthy, J., Mounir, Z., Raven, J., and Koromilas, A. (2008). The eIF2α kinases inhibit vesicular stomatitis virus replication independently of eIF2 phosphorylation. Cell Cycle *7*, 2346–2351.

Kuhn, A., Koch, H.-G., and Dalbey, R.E. (2017). Targeting and Insertion of Membrane Proteins. EcoSal Plus *7*.

Laeger, T., Albarado, D.C., Burke, S.J., Trosclair, L., Hedgepeth, J.W., Berthoud, H.-R., Gettys, T.W., Collier, J.J., Münzberg, H., and Morrison, C.D. (2016). Metabolic Responses to Dietary Protein Restriction Require an Increase in FGF21 that Is Delayed by the Absence of GCN2. Cell Reports *16*, 707–716.

Laplante, M., and Sabatini, D.M. (2009). mTOR signaling at a glance. J Cell Sci *122*, 3589–3594.

Lee, Y.S., Shibata, Y., Malhotra, A., and Dutta, A. (2009). A novel class of small RNAs: tRNA-derived RNA fragments (tRFs). Genes Dev *23*, 2639–2649.

Lesperance, D.N., and Broderick, N.A. (2020). Microbiomes as modulators of Drosophila melanogaster homeostasis and disease. Current Opinion in Insect Science *39*, 84–90.

Li, M., Lee, K., Hsu, M., Nau, G., Mylonakis, E., and Ramratnam, B. (2017). Lactobacillus-derived extracellular vesicles enhance host immune responses against vancomycin-resistant enterococci. BMC Microbiol *17*.

Lifshitz, F. (2009). Nutrition and growth. J Clin Res Pediatr Endocrinol *1*, 157–163.

Ma, X.M., and Blenis, J. (2009). Molecular mechanisms of mTOR-mediated translational

control. Nat Rev Mol Cell Biol *10*, 307–318.

Maguin, E., Prévost, H., Ehrlich, S.D., and Gruss, A. (1996). Efficient insertional mutagenesis in lactococci and other gram-positive bacteria. J Bacteriol *178*, 931–935.

Malzer, E., Szajewska-Skuta, M., Dalton, L.E., Thomas, S.E., Hu, N., Skaer, H., Lomas, D.A., Crowther, D.C., and Marciniak, S.J. (2013). Coordinate regulation of eIF2α phosphorylation by PPP1R15 and GCN2 is required during Drosophila development. J Cell Sci *126*, 1406–1415.

Malzer, E., Dominicus, C.S., Chambers, J.E., Dickens, J.A., Mookerjee, S., and Marciniak, S.J. (2018). The integrated stress response regulates BMP signalling through effects on translation. BMC Biol *16*.

Martino, M.E., Bayjanov, J.R., Caffrey, B.E., Wels, M., Joncour, P., Hughes, S., Gillet, B., Kleerebezem, M., van Hijum, S.A.F.T., and Leulier, F. (2016). Nomadic lifestyle of *Lactobacillus plantarum* revealed by comparative genomics of 54 strains isolated from different habitats. Environ. Microbiol. *18*, 4974–4989.

Masson, G.R. (2019). Towards a model of GCN2 activation. Biochem Soc Trans *47*, 1481–1488.

Matos, R.C., Schwarzer, M., Gervais, H., Courtin, P., Joncour, P., Gillet, B., Ma, D., Bulteau, A.-L., Martino, M.E., Hughes, S., et al. (2017). D-Alanylation of teichoic acids contributes to *Lactobacillus plantarum*-mediated *Drosophila* growth during chronic undernutrition. Nat Microbiol *2*, 1635–1647.

Moriano-Gutierrez, S., Bongrand, C., Essock-Burns, T., Wu, L., McFall-Ngai, M.J., and Ruby, E.G. (2020). The noncoding small RNA SsrA is released by Vibrio fischeri and modulates critical host responses. PLOS Biology *18*, e3000934.

Natarajan, K., Meyer, M.R., Jackson, B.M., Slade, D., Roberts, C., Hinnebusch, A.G., and Marton, M.J. (2001). Transcriptional Profiling Shows that Gcn4p Is a Master Regulator of Gene Expression during Amino Acid Starvation in Yeast. Molecular and Cellular Biology *21*, 4347–4368.

Niculescu, M.D., and Zeisel, S.H. (2002). Diet, Methyl Donors and DNA Methylation: Interactions between Dietary Folate, Methionine and Choline. J Nutr *132*, 2333S-2335S.

Olsen, D.S., Jordan, B., Chen, D., Wek, R.C., and Cavener, D.R. (1998). Isolation of the gene encoding the Drosophila melanogaster homolog of the Saccharomyces cerevisiae GCN2 eIF-2alpha kinase. Genetics *149*, 1495–1509.

Overend, G., Luo, Y., Henderson, L., Douglas, A.E., Davies, S.A., and Dow, J.A.T. (2016). Molecular mechanism and functional significance of acid generation in the Drosophila midgut. Sci Rep *6*, 27242.

Piper, M.D. (2017). Using artificial diets to understand the nutritional physiology of *Drosophila melanogaster*. Curr Opin Insect Sci *23*, 104–111.

Piper, M.D., Blanc, E., Leitão-Gonçalves, R., Yang, M., He, X., Linford, N.J., Hoddinott, M.P., Hopfen, C., Soultoukis, G.A., Niemeyer, C., et al. (2014). A holidic medium for Drosophila melanogaster. Nat Methods *11*.

Piper, M.D.W., Soultoukis, G.A., Blanc, E., Mesaros, A., Herbert, S.L., Juricic, P., He, X., Atanassov, I., Salmonowicz, H., Yang, M., et al. (2017). Matching dietary amino acid balance to the *in silico*-translated exome optimizes growth and reproduction without cost to lifespan. Cell Metabolism *25*, 610–621.

Redhai, S., Pilgrim, C., Gaspar, P., Giesen, L. van, Lopes, T., Riabinina, O., Grenier, T., Milona, A., Chanana, B., Swadling, J.B., et al. (2020). An intestinal zinc sensor regulates food intake and developmental growth. Nature *580*, 263–268.

Ren, B., Wang, X., Duan, J., and Ma, J. (2019). Rhizobial tRNA-derived small RNAs are signal molecules regulating plant nodulation. Science *365*, 919–922.

Rodrigues, Y.K., Bergen, E. van, Alves, F., Duneau, D., and Beldade, P. (2021). Additive and non-additive effects of day and night temperatures on thermally plastic traits in a model for adaptive seasonal plasticity. Evolution *75*, 1805–1819.

Russell, C.W., Bouvaine, S., Newell, P.D., and Douglas, A.E. (2013). Shared metabolic pathways in a coevolved insect-bacterial symbiosis. Appl. Environ. Microbiol. *79*, 6117–6123.

Ryu, J.-H., Kim, S.-H., Lee, H.-Y., Bai, J.Y., Nam, Y.-D., Bae, J.-W., Lee, D.G., Shin, S.C., Ha, E.-M., and Lee, W.-J. (2008). Innate immune homeostasis by the homeobox gene *Caudal* and commensal-gut mutualism in *Drosophila*. Science *319*, 777–782.

Saguir, F.M., and de Nadra, M.C.M. (2007). Improvement of a chemically defined medium for the sustained growth of *Lactobacillus plantarum*: nutritional requirements. Curr. Microbiol. *54*, 414–418.

Sakaguchi, E. (2003). Digestive strategies of small hindgut fermenters. Animal Science Journal *74*, 327–337.

Sang, J.H. (1956). The quantitative nutritional requirements of *Drosophila melanogaster*. Journal of Experimental Biology *33*, 45–72.

Sannino, D.R., Dobson, A.J., Edwards, K., Angert, E.R., and Buchon, N. (2018). The *Drosophila melanogaster* gut microbiota provisions thiamine to its host. MBio *9*, e00155-18.

Schindelin, J., Arganda-Carreras, I., Frise, E., Kaynig, V., Longair, M., Pietzsch, T., Preibisch, S., Rueden, C., Saalfeld, S., Schmid, B., et al. (2012). Fiji: an open-source platform for biological-image analysis. Nat Methods *9*, 676–682.

Schwarzer, M., Makki, K., Storelli, G., Machuca-Gayet, I., Srutkova, D., Hermanova, P., Martino, M.E., Balmand, S., Hudcovic, T., Heddi, A., et al. (2016). *Lactobacillus plantarum* strain maintains growth of infant mice during chronic undernutrition. Science *351*, 854–857.

Schwarzer, M., Strigini, M., and Leulier, F. (2018). Gut Microbiota and Host Juvenile Growth. Calcified Tissue International *102*, 387–405.

Selosse, M.-A., Bessis, A., and Pozo, M.J. (2014). Microbial priming of plant and animal immunity: symbionts as developmental signals. Trends in Microbiology *22*, 607–613.

Shin, S.C., Kim, S.-H., You, H., Kim, B., Kim, A.C., Lee, K.-A., Yoon, J.-H., Ryu, J.-H., and Lee, W.-J. (2011). *Drosophila* microbiome modulates host developmental and metabolic homeostasis via insulin signaling. Science *334*, 670–674.

Staubach, F., Baines, J.F., Künzel, S., Bik, E.M., and Petrov, D.A. (2013). Host Species and Environmental Effects on Bacterial Communities Associated with Drosophila in the Laboratory and in the Natural Environment. PLOS ONE *8*, e70749.

Storelli, G., Defaye, A., Erkosar, B., Hols, P., Royet, J., and Leulier, F. (2011). *Lactobacillus plantarum* promotes *Drosophila* systemic growth by modulating hormonal signals through TOR-dependent nutrient sensing. Cell Metab. *14*, 403–414.

Storelli, G., Strigini, M., Grenier, T., Bozonnet, L., Schwarzer, M., Daniel, C., Matos, R., and Leulier, F. (2018). *Drosophila* perpetuates nutritional mutualism by promoting the fitness of its intestinal symbiont *Lactobacillus plantarum*. Cell Metab *27*, 362-377.e8.

Tattoli, I., Sorbara, M.T., Vuckovic, D., Ling, A., Soares, F., Carneiro, L.A.M., Yang, C., Emili, A., Philpott, D.J., and Girardin, S.E. (2012). Amino Acid Starvation Induced by Invasive Bacterial Pathogens Triggers an Innate Host Defense Program. Cell Host & Microbe *11*, 563–575.

Tennessen, J.M., and Thummel, C.S. (2011). Coordinating growth and review maturation — insights from *Drosophila*. Curr Biol *21*, R750–R757.

Teske, B.F., Baird, T.D., and Wek, R.C. (2011). Chapter Nineteen - Methods for Analyzing eIF2 Kinases and Translational Control in the Unfolded Protein Response. In Methods in Enzymology, P.M. Conn, ed. (Academic Press), pp. 333–356.

Teusink, B., van Enckevort, F.H.J., Francke, C., Wiersma, A., Wegkamp, A., Smid, E.J., and Siezen, R.J. (2005). *In silico* reconstruction of the metabolic pathways of *Lactobacillus plantarum*: comparing predictions of nutrient requirements with those from growth experiments. Appl Environ Microbiol *71*, 7253–7262.

Therneau, T.M., and Grambsch, P.M. (2000). Modeling Survival Data: Extending the Cox Model (New York: Springer-Verlag).

Vandehoef, C., Molaei, M., and Karpac, J. (2020). Dietary Adaptation of Microbiota in Drosophila Requires NF-κB-Dependent Control of the Translational Regulator 4E-BP. Cell Rep *31*, 107736.

Vasudevan, D., Clark, N.K., Sam, J., Cotham, V.C., Ueberheide, B., Marr, M.T., and Ryoo, H.D. (2017). The GCN2-ATF4 signaling pathway induces 4E-BP to bias translation and boost antimicrobial peptide synthesis in response to bacterial infection. Cell Reports *21*, 2039–2047.

Wek, R.C., and Cavener, D.R. (2007). Translational Control and the Unfolded Protein Response. Antioxidants & Redox Signaling *9*, 2357–2372.

Wek, S.A., Zhu, S., and Wek, R.C. (1995). The histidyl-tRNA synthetase-related sequence in the eIF-2 alpha protein kinase GCN2 interacts with tRNA and is required for activation in response to starvation for different amino acids. Mol Cell Biol *15*, 4497–4506.

West, C.L., Stanisz, A.M., Mao, Y.-K., Champagne-Jorgensen, K., Bienenstock, J., and Kunze, W.A. (2020). Microvesicles from Lactobacillus reuteri (DSM-17938) completely reproduce modulation of gut motility by bacteria in mice. PLOS ONE *15*, e0225481.

Wong, S.Y., Javid, B., Addepalli, B., Piszczek, G., Strader, M.B., Limbach, P.A., and Barry, C.E. (2013). Functional role of methylation of G518 of the 16S rRNA 530 loop by GidB in Mycobacterium tuberculosis. Antimicrob. Agents Chemother. *57*, 6311–6318.

Wu, G. (2009). Amino acids: metabolism, functions, and nutrition. Amino Acids *37*, 1–17.
Yamada, R., Deshpande, S.A., Bruce, K.D., Mak, E.M., and Ja, W.W. (2015). Microbes promote amino acid harvest to rescue undernutrition in *Drosophila*. Cell Rep.

Zhang, P., McGrath, B.C., Reinert, J., Olsen, D.S., Lei, L., Gill, S., Wek, S.A., Vattem, K.M., Wek, R.C., Kimball, S.R., et al. (2002). The GCN2 eIF2α Kinase Is Required for Adaptation to Amino Acid Deprivation in Mice. Mol Cell Biol *22*, 6681–6688.

Zhu, S., and Wek, R.C. (1998). Ribosome-binding Domain of Eukaryotic Initiation Factor-2 Kinase GCN2 Facilitates Translation Control *. Journal of Biological Chemistry *273*, 1808–1814.